AD_____

CONTRACT NUMBER DAMD17-93-C-3100

TITLE: Mechanism of Botulinum Toxin a Neurotoxicity: Channel Formation and Protein Phosphorylation

PRINCIPAL INVESTIGATOR: Mauricio Montal, M.D., Ph.D.

CONTRACTING ORGANIZATION: University of California, San Diego
La Jolla, California 92093-0934

REPORT DATE: March 1997

TYPE OF REPORT: Final

PREPARED FOR: Commander
U.S. Army Medical Research and Materiel Command
Fort Detrick, Frederick, Maryland 21702-5012

REPORT DOCUMENTATION PAGE

Form Approved
OMB No. 0704-0188

1. AGENCY USE ONLY *(Leave blank)*	2. REPORT DATE	3. REPORT TYPE AND DATES COVERED
	March 1997	Final (30 Apr 93 - 31 Jan 97)

4. TITLE AND SUBTITLE
Mechanism of Botulinum Toxin a Neurotoxicity: Channel Formation and Protein Phosphorylation

5. FUNDING NUMBERS
DAMD17-93-C-3100

6. AUTHOR(S)
Mauricio Montal, M.D., Ph.D.

7. PERFORMING ORGANIZATION NAME(S) AND ADDRESS(ES)
University of California, San Diego
La Jolla, California 92093-0934

8. PERFORMING ORGANIZATION REPORT NUMBER

9. SPONSORING/MONITORING AGENCY NAME(S) AND ADDRESS(ES)
Commander
U.S. Army Medical Research and Materiel Command
Fort Detrick, Frederick, MD 21702-5012

10. SPONSORING/MONITORING AGENCY REPORT NUMBER

11. SUPPLEMENTARY NOTES

12a. DISTRIBUTION / AVAILABILITY STATEMENT
Approved for public release; distribution unlimited

12b. DISTRIBUTION CODE

13. ABSTRACT *(Maximum 200*

A unique contribution of this program is the discovery of potentiation of botulinum neurotoxin (BoTx) A protease activity by tyrosine phosphorylation. This key finding underscores the requirement to screen for potential blockers using the pharmacologically relevant target, namely tyrosine phosphorylated neurotoxin, presumably the biologically active form within the cells. A most exciting outcome is the ability to design peptides that selectively block neurotransmitter release. The proteolytic products of the BoTx activity have proved to be instrumental in providing clues about the secretory vesicle fusion process. These peptides are suitable mimics of the neurotoxin itself, displaying effective inhibitory activity on transmitter release by inhibiting vesicle docking and thereby disabling the fusion machinery. Peptides designed along these principles may find clinical application as BoTx substitutes in the treatment or management of disorders associated with involuntary muscle spasms. A major finding is the identification of an ion channel-forming motif in BoTxA heavy chain. The ion channel activity of BoTx may be abrogated by identifying effective open channel blockers, lending credence to the concept that open channel blockers may be a single class of drugs effective against all BoTxs isoforms. The potency of such agents may, in principle, be augmented by combining active compounds against both the protease and channel activities of the neurotoxin which are considered necessary for its neurotoxicity.

14. SUBJECT TERMS	15. NUMBER OF PAGES
botulinum neurotoxin; protein phosphorylation; vesicle fusion; ion channels; inhibitors of neurosecretion; synaptic transmission.	40
	16. PRICE CODE

17. SECURITY CLASSIFICATION OF REPORT	18. SECURITY CLASSIFICATION OF THIS PAGE	19. SECURITY CLASSIFICATION OF ABSTRACT	20. LIMITATION OF ABSTRACT
Unclassified	Unclassified	Unclassified	Unlimited

FOREWORD

Opinions, interpretations, conclusions and recommendations are those of the author and are not necessarily endorsed by the U.S. Army.

____ Where copyrighted material is quoted, permission has been obtained to use such material.

____ Where material from documents designated for limited distribution is quoted, permission has been obtained to use the material.

____ Citations of commercial organizations and trade names in this report do not constitute an official Department of Army endorsement or approval of the products or services of these organizations.

✓ In conducting research using animals, the investigator(s) adhered to the "Guide for the Care and Use of Laboratory Animals," prepared by the Committee on Care and use of Laboratory Animals of the Institute of Laboratory Resources, national Research Council (NIH Publication No. 86-23, Revised 1985).

____ For the protection of human subjects, the investigator(s) adhered to policies of applicable Federal Law 45 CFR 46.

____ In conducting research utilizing recombinant DNA technology, the investigator(s) adhered to current guidelines promulgated by the National Institutes of Health.

____ In the conduct of research utilizing recombinant DNA, the investigator(s) adhered to the NIH Guidelines for Research Involving Recombinant DNA Molecules.

✓ In the conduct of research involving hazardous organisms, the investigator(s) adhered to the CDC-NIH Guide for Biosafety in Microbiological and Biomedical Laboratories.

M. Morris 2/12/97

PI - Signature Date

TABLE OF CONTENTS

INTRODUCTION

This study examined different mechanisms for the action and modulation of botulinum neurotoxin (BoTx)*A light chain (LC) that focus on the notion that it acts by inhibiting exocytosis at the level of vesicle fusion with the presynaptic plasma membrane, and identifies the minimum and specific sequence contained in the heavy chain (HC) that is responsible for the ion channel activity. Powerful new approaches are used in concert to understand this fundamental question. The results of this program are contributing towards the development of a structure-function map of BoTxA that may lead to strategies to prevent or relieve the transmitter release blockade exerted at nerve terminals that accounts for its neuroparalytic toxic action.

Clostridial neurotoxins produced by *Clostridium botulinum* and *Clostridium tetani* are some of the most potent neuroparalytic agents known to man and the causative agents of botulism and tetanus (1,2). Paradoxically, BoTx A is also an effective therapeutic agent for certain neuromuscular disorders associated with muscle spasms such as strabismus and dystonias (3). BoTxA and its related serotypes produce flaccid paralysis in skeletal muscles by blocking exocytotic acetylcholine release at the neuromuscular junction (1,2).

Botulinum neurotoxins are soluble proteins, produced by the bacteria as a single chain of M_r 150,000 (1,2). The holotoxin undergoes proteolytic cleavage yielding a fully active dichain polypeptide composed of a heavy chain, M_r 100,000, and a light chain, M_r 50,000, linked by a disulfide bond. The LCs of these neurotoxins are Zn^{2+}-metalloproteases that selectively cleave proteins involved in targeting to and fusion with the plasma membrane of presynaptic vesicles, thereby blocking neurotransmitter release into the synaptic cleft (4-13). A Zn^{2+}-binding motif characteristic of a family of Zn^{2+}-endopeptidases has been identified in the LC of the seven isoforms of BoTx and of TeTx. The consensus sequence is: DPALTLMHELIHALHGLYG (13-15).

Recent studies on the biochemical dissection of the components involved in the fusion of secretory vesicles with the plasma membrane have set BoTxs at the center of this process. The information accrued in recent years has led to the formulation of the **SNAP receptors** (SNARE) model to describe the final steps of the secretion cascade (15-24). The SNARE hypothesis distinguishes three distinct stages in the pathway, namely docking, priming and fusion. Vesicle docking refers to the process by which cargo vesicles are targeted to the plasma membrane at the active zone, although they are not competent for Ca^{2+}-triggered fusion (4). After docking, vesicles are activated by an ATP-dependent step known as vesicle priming. Primed vesicles are readily releasable in response to a transient Ca^{2+} elevation that triggers the fusion event.

Biochemically, docking is associated with the formation of a 7S ternary complex involving the vesicle membrane protein synaptobrevin, also known as vesicle associated membrane protein (VAMP) which is the vesicle SNARE (v-SNARE), and two plasma membrane proteins SNAP-25 and syntaxin which comprise the target SNARE (t-SNARE) (17-27). Vesicle priming is initiated by binding of the soluble proteins NSF (for N-ethylmaleimide-sensitive factor, an ATPase) and SNAPs (for soluble NSF attachment proteins, which are not related to SNAP-25) to the SNAP receptors (4,23). Specifically, VAMP binds to the SNAP-25-syntaxin heterodimer forming a ternary core complex that serves as a receptor for SNAPs and recruits NSF forming a 20S complex (17-21,24-29). ATP-hydrolysis by bound NSF energizes the secretory vesicles to the primed state, in which they are ready to fuse with the plasma membrane and release their content in response to the Ca^{2+} signal (16-23,30). The identification of an ATP-dependent, slow component in the final steps of the exocytotic cascade lends support to the SNARE hypothesis.

The discovery that *Clostridial* neurotoxins target specific components of the v-SNARE and t-SNARE has contributed to our knowledge of the molecular entities comprising the exocytotic machinery, as well as the molecular events involved in Ca^{2+}-mediated neuroexocytosis. Botulinum

neurotoxins B, D, F, and G, and the structurally related tetanus toxin specifically cleave VAMP at different sites (6,15,31,32), whereas BoTxA and E cleave SNAP-25 at the C-teminus (11,12,33), and BoTx C cuts syntaxin and SNAP-25 (34-36). Cleavage of any of these proteins prevents the formation of the core complex and abrogates Ca^{2+}-triggered exocytosis (4,5,15,18,23).

As summarized on page 10, during the current funding period, we discovered that synthetic peptides patterned after the amino acid sequence of C-terminal segments from SNAP-25 (37-39) are specific inhibitors of neurosecretion. These peptides, for which the term ESUP (Excitation Secretion Uncoupling Peptides) was coined to highlight their activity (37), are useful pharmacological tools to probe the functional role of distinct protein components in the secretory machinery, to dissect the contribution of specific domains in the protein-protein interactions that mediate the process, and to identify steps in the exocytotic cascade. Peptides that imitate segments from synaptotagmin (40,41), SNAPs (42), and synaptobrevin (43) have also been reported to act as inhibitor of neurosecretion. The use of this new set of reagents, however, remains limited because the mechanism underlying their inhibitory activity is unknown. Therefore, as described on page 10, we characterized the molecular steps of the exocytotic process that are sensitive to the blocking activity of a 20-mer peptide that mimics the amino acid sequence of the C-terminal domain of SNAP-25 (SNAP-25(187-206): SNKTRIDEANQRATKMLGSG; denoted as ESUP-A. We showed that ESUP-A arrests Ca^{2+}-dependent secretion from permeabilized chromaffin cells by inhibiting vesicle docking.

Protease activity is not sufficient to account for the long term (several days) paralytic effects exerted by BoTxA nor the potentiation of its neurotoxicity by external stimuli that elevate the intracellular Ca^{2+} concentration (1-3, 44-50). These facts hint important differences between the *in vitro* and *in vivo* forms of the toxin implying potential modulation of the neurotoxins by intracellular regulatory processes, such as protein phosphorylation.

As summarized on page 13, during the current funding period, we discovered that *Clostridial* neurotoxins are substrates of protein tyrosine kinases, that tyrosine phosphorylation produces a prominent augmentation of their proteolytic activity and thermal stability, and proposed that the phosphorylated form of these neurotoxins may be the physiological active species within cells (51). Demonstration of intracellular tyrosine phosphorylation of the neurotoxin by selective stimulation of neuroendocrine cells underscores that tyrosine phosphorylation may indeed be a missing link in the biology of *Clostridial* neurotoxins (51).

BoTxs LC is disulfide linked to a heavy chain, M_r 100 kD, which is necessary for toxin internalization (13,15). BoTxs have an inherent propensity to insert into membranes, especially at acidic pH (cf.13). This property is compatible with the ion channel activity observed when BoTxA, B, C, D and E are reconstituted in lipid bilayers (52-54). It has been proposed that such a channel is the conduit through which the LC gets access to the cytosol where it acts (52-55). The finding that all these intracellularly acting toxins enter cells by endocytosis, has suggested that the acid pH of endocytic vesicles induces a conformational change that promotes insertion of the HC of the toxins into and across the endosomes, therefore allowing the translocation of the LC catalytic moiety into the cytosol where it acts (1,13,15,52-61). This model implies that toxin translocation and channel formation are related phenomena (62).

The amino-terminal domain of the HC appears involved in membrane insertion and translocation (for reviews see 13,15), and contains the channel-forming activity of BoTxA (54). Sequence analysis suggests the occurrence in this domain of an amphipathic stretch sufficiently long to span the width of the bilayer as a transmembrane helix (63,64). Conformational energy calculations suggest that such a motif is thermodynamically feasible and compatible with the assembly of a transmembrane channel by the clustering of four α-helices (63). Image reconstruction analysis of electronmicrographs of BoTx inserted in membranes suggests the

occurrence of a tetramer as the structural entity underlying the BoTx channel (65). As summarized on page15, during the current funding period, we discovered that a peptide with a sequence corresponding to the amphipathic segment of BoTxA HC indeed forms ion channels in lipid bilayers (66).

Thus, in spite of the absence of a high resolution structure of botulinum neurotoxin A, two functional modules have been uncovered in the protein sequence: A Zn^{2+}-binding motif associated with the metalloprotease activity of the light chain; the second, an amphipathic α-helical transmembrane motif associated with the ion-channel activity of the heavy chain. Further, tyrosine phosphorylation produces a prominent augmentation of the BoTx proteolytic activity and thermal stability suggesting that the phosphorylated form of these neurotoxins may be the physiological active species within cells. Identification of these modules and demonstration of modulation by tyrosine phosphorylation suggests specific mechanisms for the neuroparalytic action of BoTxs and provides opportunities for pharmacological intervention in botulinum neurotoxicity.

BODY

EXPERIMENTAL METHODS

1. Peptide synthesis, purification and characterization

Peptides were synthesized by solid-phase methods using an Applied Biosystems Model 431 peptide synthesizer (ABI, Foster City, CA) and purified by reversed-phase HPLC (63,66). The purified peptides were analyzed by electrospray ionization mass spectrometry using a triple quadrupole mass spectrometer (Model API III, Sciex, Thornhill, Ontario, Canada); ionization was done at a flow rate of 4 μl/min, as described (66).

2. Reconstitution in lipid bilayers and single channel recordings

Lipid bilayers were formed at the tip of patch pipets by apposition of two monolayers (58,59,61,63,66). Lipid monolayers were spread from a lipid solution in hexane (5 mg/ml); the lipids were 4:1 POPE/POPC [1-palmitoyl-2-oleoyl-*sn*-glycero-3-phosphoethanolamine (POPE) and 1-palmitoyl-2-oleoyl-*sn*-glycero-3-phosphocholine (POPC)] (Avanti Biochemicals, Alabaster, AL). Peptides were dissolved in trifluoroethanol (TFE) and added to the aqueous subphase after bilayer formation to the final concentration indicated in figure legends. The aqueous subphase was composed of 0.5 M KCl or NaCl, 1 mM $CaCl_2$ and 5 mM Hepes (pH 7.4). Bilayer experiments were performed at 24 ± 2 °C. Acquisition and analysis of single channel currents were as described (58,59,61,63,66). Records were filtered with an 8-pole Bessel filter (Frequency Services, Haverhill, MA) and digitized at 0.5 ms sampling interval using an Axon TL-1 interface (Axon Instruments, Burlingame, CA) connected to a PC. pClamp 5.5 package (Axon Instruments) was used for data processing. The channel recordings illustrated are representative of the most frequently observed conductances under the given salt and concentration conditions. Single channel conductance, γ, was calculated from Gaussian fits to currents histograms and channel open (τ_o) and closed (τ_c) lifetimes calculated from exponential fits to probability density functions (59,63,66). Openings with $\tau_o \leq 0.3$ ms were ignored. n denotes number of experiments and N, number of events. γ, τ_o, and τ_c were calculated from segments of continuous recordings lasting t > 45 sec and with $N \geq 500$ events; data from different experiments are reported as mean ± SEM. The data reported include statistical analysis of 7,000 single channel openings.

3. Conformational energy computations

Molecular modeling, including energy minimization and molecular dynamics simulations, were conducted on a *Silicon Graphics IRIS 4D/21 GTX workstation* using the INSIGHT and DISCOVER molecular modeling packages of Biosym (San Diego, CA) (63,66). Low-energy arrangements of α-helices and four-helix bundles are calculated with semi-empirical potential energy functions and optimization routines, and further refined. Constraints are used for

symmetry and to maintain regular helical backbone dihedral angles of $\phi = -45°$ and $\psi = -60°$ (66).

4. Purification of clostridial neurotoxins

Botulinum toxins were purified and activated as described (50): 50 µg (200 µl) of ammonium sulfate precipitated BoTxA were centrifuged at 14,000 rpm in an Eppendorf centrifuge. The pellet was resuspended in 50 µl of 20 mM NaH_2PO_4, 150 mM NaCl pH 7.4 buffer and dialyzed against the same buffer for 2 h at 5 °C. Dialysis was performed in a Pierce System 100 Microdialyzer, using 1,000 daltons M_r cutoff dialysis membranes (Pierce Co., Rockford, IL). Toxin was activated by incubation in 10 mM DTT for 30 min at 37° C.

5. Phosphorylation and dephosphorylation of clostridial neurotoxins

The tyrosine phosphorylation reaction (final volume of 20-40 µl) contained 20 mM $MgCl_2$, 1 mM EGTA, 1 mM DTT, 20 mM Hepes (pH 7.4), 3-6 Units of Src kinase (UBI), 0.1 mM ATP and 4 µCi [γ-^{32}P] ATP (3,000 Ci/mmol). Reactions proceed at 30 °C for the indicated times and were terminated by addition of SDS-PAGE sample buffer or 200 µM peptide A (Peninsula), a specific inhibitor of Src (51). PKC (20 ng; UBI) phosphorylation buffer was: 20 mM Hepes, pH 7.4, 0.1 mM $CaCl_2$, 10 mM $MgCl_2$, 0.25 mg/ml L-α-phosphatidyl-L-serine and 1 mM DTT. Phosphorylation by PKA (4 U; Sigma) was as described (51). Phosphorylated samples subjected to SDS-PAGE on 12% gels were stained with Coomassie blue R-250, destained, dried and exposed to Kodak X-Omat AR x-ray film. Dephosphorylation reactions (15 µl) contained 100 nM tyrosine-phosphorylated BoTxA and 50 ng PTP-1B-agarose conjugate (UBI). Reactions proceed at 37°C for indicated times, and were terminated by centrifugation at 14,000 rpm, 1 min. The extent of BoTxA dephosphorylation was assessed by SDS-PAGE and autoradiography.

6.Western blot and immunoprecipitation analysis

For immunoblots, protein bands were electrotransferred onto nitrocellulose membranes, and blocked with 3% BSA (51). Proteins were detected using the ECL system. For immunoprecipitation assays, cells were stimulated with PBS supplemented with indicated additives, washed with cold PBS, lysed with cold RIPA buffer (50 mM Tris-HCl pH 7.4, 150 mM NaCl, 1% Nonidet P40, 0.25% deoxycholate, 1 mM EGTA, 1 mM NaF, 1 mM Na_3VO_4, 1 µg/ml leupeptine, 1 µg/ml pepstatine A and 1 mM phenylmethylsulfonylfluoride, incubated and shaked at 4°C for 25 min. Insoluble material was removed by centrifugation at 10,000 x *g* for 30 min at 4°C. Soluble material was analyzed by immunoblot or used for immunoprecipitation. Tyrosine-phosphorylated proteins were immunoprecipitated with antiphosphotyrosine mAb (clone 4G10; UBI) (4 µg mAb/mg protein). Immunocomplexes were captured with agarose-conjugated protein G (75 µl; Pierce), and washed six times with 500 µl of RIPA buffer at 4°C. Immunoprecipitates were dissolved in 50 µl of SDS-PAGE buffer, boiled 5 min and analyzed by SDS-PAGE and immunoblotting. Blots were probed with anti-BoTxA LC mAb#9 and anti-BoTxA HC mAb#6. Bands were visualized using the ECL system.

7. In vitro cleavage of SNAP-25

In vitro translation of the cDNA clone coding for SNAP-25 from mouse brain (51) in the presence of [^{35}S]methionine (Amersham) involved a transcription-translation-coupled reticulocyte lysate system (Promega). Cleavage assay was conducted at 30°C using BoTxA at the indicated concentrations. Samples were analyzed by SDS-PAGE followed by fluorographic detection, and quantitated using the public domain NIH Image program v1.57.

8. Cell culture

Rat pheochromocytoma PC12 cells were propagated in RPMI 1640 medium, supplemented with 10% donor horse serum-5% bovine fetal serum, at 37°C in a humidified incubator with 5% CO_2 (51). For NGF differentiation (50 ng/ml, for 4 days; GIBCO), PC12 cells were plated at a density of 10^6 cells/ml on 75 cm^2 culture dishes coated with rat tail collagen (51). For intracellular neurotoxin phosphorylation experiments, cells were incubated with 100 nM BoTxA dissolved in

PBS for 12 h at 37°C, 5% CO_2.Chromaffin cells were prepared from bovine adrenal glands by collagenase digestion and further separated from debris and erythrocytes by centrifugation on Percoll gradients as described (37,38). Cells were maintained in monolayer cultures at a density of 625,000 cells/cm^2 and were used between the third and sixth day after plating. All the experiments were performed at 37 °C.

9. Determination of catecholamine release from detergent-permeabilized chromaffin cells Secreted [^{3}H]noradrenaline was determined in digitonin-permeabilized cells as described (37,38). Briefly, cells were incubated with [^{3}H]noradrenaline (1 μCi/ml) in DMEM supplemented with 0.56 mM ascorbic acid during 4 h. Thereafter, monolayers were washed 4 times with a Krebs/HEPES basal solution: 15 mM Hepes pH 7.4 with 134 mM NaCl, 4.7 mM KCl, 1.2 mM KH_2PO_4, 1.2 mM $MgCl_2$, 2.5 mM $CaCl_2$, 0.56 mM ascorbic acid and 11 mM glucose. Cell permeabilization was accomplished with 20 μM digitonin in 20 mM Pipes, pH 6.8 with 140 mM monosodium glutamate, 2 mM $MgCl_2$, 2 mM Mg-ATP, and 5 mM EGTA. This incubation was carried out in the absence or presence of 100 mM ESUP-A, ESUP-A^{RDM}, or 100 nM dithiothreitol (DTT)-reduced BoTxA as indicated. BoTxA was reduced with 10 mM DTT for 30 min at 37°C. Following permeabilization, media were discarded and cells were incubated for 10 additional min in digitonin-free medium in presence or absence of peptides. Basal secretion was measured in 5 mM EGTA, whereas stimulated secretion was measured in a medium containing 10 μM buffered Ca^{2+} solution. Media were collected and released catecholamines as well as the total cell content were determined by liquid scintillation counting. Statistical significance was calculated using Student *t*-test with data from 4 or more independent experiments.

10. Electron microscopy of permeabilized chromaffin cells.- Chromaffin cells (10^6 cells/well) were permeabilized and peptide (100 μM) or DTT-reduced BoTxA (100 nM) incubated as described above. Cells were collected by low speed centrifugation (1000xg for 2 min) and fixed with 2.5% glutaraldehyde, 2% paraformaldehyde in 0.05 M cacodylate buffer at pH 7.3 for 2 h. The pellets were postfixed in 1.33% osmic acid during 1.5 h, in s-collidine buffer for ≥2 h, dehydrated, and embedded in Epon (38). Thin sections (~0.5 mm) were obtained using a Reichert Ultracut-E ultramicrotome (Vienna, Austria). Electron microscopy was performed using a transmission electron microscope (Zeiss EM-10, Oberkochem, Germany).

Vesicle density distribution was estimated in digitized micrographs using the NIH Image analysis program. For each chromaffin cell, the distance between the dense core granules and the plasma membrane was measured and binned using a bin-width of 0.15 μm. To obtain a distance distribution histogram, the number of granules occurring at given point was plotted as a function of the average distance between the plasma membrane, defined at 0 μm, and the nuclear membrane, at ~3 μm. Data are given as mean with number of cells n≥5 for each treatment; the number of vesicles (v) counted per cell was 240≤v≤290, and the experimental error 10%≤e≤15%.

MATERIALS:

The following materials were kindly provided by the investigators listed:
BoTxA and BoTxE (B.R. DasGupta, University of Wisconsin); SNAP-25, cDNA for SNAP-25 and anti-SNAP-25 polyclonal antibody (M.C. Wilson, Research Institute, Scripps Clinic); anti-SNAP-25 monoclonal antibody (Sternberger Monoclonals Inc. Baltimore, MD); anti-VAMP antibody (R. Jahn, Yale University).

RESULTS

DESIGN OF PEPTIDE INHIBITORS OF NEUROSECRETION

ESUP Concept

SNAP-25 is cleaved at single sites along its C-terminal domain by BoTxA and BoTxE (9,11). This cleavage is sufficient to disable the fusion process that leads to secretion by inhibiting vesicle docking (4,5,17,18,23,24). Presumably, the C-terminal domain of SNAP-25 is required for the competent attachment of the fusion complex to the plasma membrane that precedes the actual fusion event. This implies that synthetic peptides designed to mimic the sequences of the C-terminal domain of SNAP-25 may inhibit neurosecretion. In other words, the peptide uncouples excitation from secretion. We therefore proposed the term ESUP for the excitation-secretion uncoupling peptide (37). If this concept were demonstrated to be generally valid it would predict that peptides designed to mimic putative sequences that bind to complementary partner sequences on interacting proteins of the fusion complex may abrogate vesicle fusion and transmitter release. It is anticipated that additional ESUPs for synaptobrevin and syntaxin (40-43) and other components of the fusion complex may be identified.

Demonstration of Principle and Activity

A 20-mer peptide that mimics the C-terminal domain of SNAP-25 effectively blocks the Ca^{2+}-dependent release of catecholamines from adrenal chromaffin cells without affecting the constitutive exocytotic pathway (37). This is illustrated in Fig 1.

The peptide concentration required for half-maximal inhibition of Ca^{2+}-dependent release of noradrenaline is 30 μM. This effect is sequence specific, since a peptide with the same amino acid composition yet randomized sequence (ESUP-A^{RDM}) is inert. Inhibition requires a minimum peptide length suggesting a structural constraint to support an active conformation. The blocking effect mimics that exerted by the LC of BoTxA and E.

Mechanism Of ESUP Action: Inhibition Of Secretory Vesicle Docking

Ca^{2+}-evoked exocytosis from permeabilized chromaffin cells can be kinetically dissected in two distinct components (67,68): A fast component that may be detected few seconds after Ca^{2+} application, lasts ~1 min, and releases ~40% of the total [^{3}H]NE, followed by a slow component that proceeds for ~15 min. This biphasic behavior of catecholamine release has been associated with the presence of at least two distinct pools of secretory granules at different stages of the exocytotic cascade (18-21,69). The fast component appears to represent the release of neurotransmitter from a population of primed, readily releasable vesicles, whereas the slow component corresponds to a pool of docked vesicles that must undergo priming prior to fusion, and other releasable pools of non-docked granules (16-21,67,69). Incubation of permeabilized chromaffin cells with 100 μM ESUP-A inhibited ~60% of catecholamine release by primarily altering the slow phase of secretion. These data suggest that the pool of primed vesicles is insensitive to the action of ESUP-A (38).

To gain further insights on the specific secretory step inhibited by ESUP-A, we attempted to dissociate the two distinct components of the exocytotic process by performing a double Ca^{2+}-pulse secretion assay. The rationale considered that a short (2 min) Ca^{2+}-pulse would primarily deplete the pool of primed vesicles, with minor effects on docked vesicles. A subsequent longer (10 min) Ca^{2+} pulse would induce docking, priming and fusion of other vesicle pools. As illustrated in Fig 2, a short Ca^{2+}-pulse triggered significant exocytosis of [^{3}H]NE from chromaffin cells that is highly insensitive to 100 μM ESUP-A (~10% inhibition). In contrast, ESUP-A

blocked ~80% of the Ca^{2+}-dependent exocytosis elicited by the second, longer Ca^{2+} pulse. A synthetic peptide with the same amino acid composition, yet random sequence (ESUP-A^{RDM}) blocked only ~10% of the Ca^{2+}-evoked neurosecretion, confirming that the ESUP-A inhibitory activity is sequence specific. Taken together, these data suggest that ESUP-A inhibits Ca^{2+}-evoked catecholamine secretion by preventing vesicle docking or priming at the active zone, yet do not argue in favor of one or the other (38).

Catecholamine release from chromaffin cells is an energy-dependent process requiring ATP hydrolysis to induce and stabilize the primed state of secretory vesicles before the Ca^{2+}-induced fusion event (16-22,67,68). Vesicle priming is composed primarily of an ATP-dependent component followed by a temperature-sensitive step that leads to the Ca^{2+}-induced exocytosis (68-70). As shown in Fig 3, incubation of permeabilized chromaffin cells with 100 μM of ESUP-A attenuated ~60% of the Ca^{2+}-induced catecholamine secretion when 2 mM ATP was present in the incubation and stimulation media. The inhibitory effect was sequence specific as evidenced by the inertness of ESUP-A^{RDM}. Removal of ATP from the incubation and stimulation media diminished ~40% of the Ca^{2+}-evoked release of [^{3}H]NE (68-70). Note that the ATP-independent secretion was not affected by ESUP-A. As expected, ESUP-A did not affect the temperature-sensitive step that follows the ATP-dependent transition (data not shown). These findings suggest that ESUP-A interferes with the steps that precede the ATP-dependent activation of secretory vesicles (38).

The morphology of secretory granules in chromaffin cells treated with peptides was examined by electron microscopy (Fig 4). A main goal was to detect changes in secretory granule distribution induced by ESUP-A. For comparison purposes, the effect of BoTxA, known to prevent vesicle docking (71,72), was investigated. Electron micrographs of permeabilized, unstimulated chromaffin cells display a random distribution of dense core secretory vesicles (Fig 4A). Ca^{2+}-stimulation induces a significant depletion of granules as evidenced by the reduced number of vesicles in the cytosol (Fig 4B), in accord with other reports (69). Notably, the presence of ESUP-A produced an accumulation of vesicles near the plasma membrane (Fig 4C), similar to that produced by BoTxA (Fig 4D) (38).

Frequency distribution histograms show that unstimulated (control) chromaffin cells are characterized by the occurrence of two populations of cargo vesicles: a predominant population with a mean distance to the plasma membrane of ~0.5 μm, and a second most frequent with a mean distance of ~2.3 μm. Ca^{2+}-stimulated exocytosis in control cells or cells incubated with 100 μM ESUP-A^{RDM} decreased the total number of vesicles, as evidenced by the reduction in the area of both granule populations. By contrast, treatment with 100 μM ESUP-A or 100 nM BoTxA notably skewed the distribution of vesicles towards the plasma membrane, resulting in the virtual disappearance of the population centered at ~2.3 μm and the ensuing increase of the granule population centered at ~0.5 μm. The majority of vesicles gathered at the active zone, however, are not in tight contact with the membrane, lending support to the notion that ESUP-A prevents vesicle docking (38).

Thus, the 20-mer peptide that mimics the C-terminus of SNAP-25, effectively inhibits Ca^{2+}-dependent exocytosis in endocrine cells by preventing the docking of cargo vesicles at the plasma membrane. Our results with ESUP-A are compatible with the concept that the peptide prevents the formation of the docked state and the ensuing intermediates in the exocytotic pathway. The finding that ESUP-A does not affect the fast, ATP-independent, Ca^{2+}-mediated component suggests that its site of action is upstream of the fusion event. That ESUP-A abrogates the slow, ATP-dependent (B⇒C) component is consistent with an inhibition of the formation of the primed state C, either by blocking the transition from the docked state B to the first step of the priming process or by inhibiting vesicle docking. The observation that ESUP-A promotes a massive accumulation of secretory vesicles near the plasma membrane of chromaffin cells, but not in tight contact, implies that the peptide blocks the formation of the docked state. This mechanism of action of ESUP (38) is similar to that proposed for BoTxA (71,72):

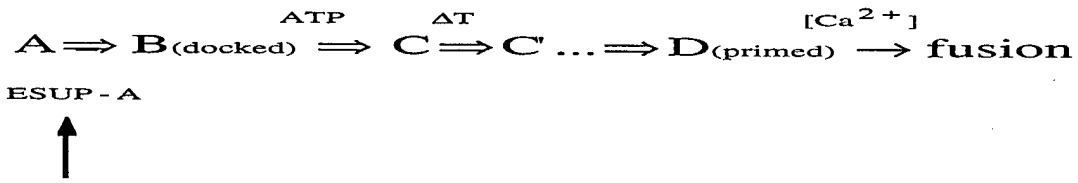

How does ESUP-A prevent vesicle docking? During docking, a ternary complex involving VAMP, SNAP-25 and syntaxin is formed, the so-called SDS-resistant complex (17-21,73). A sequence of protein-protein interactions starts with binding of SNAP proteins to the ternary aggregate and recruitment of NSF. The next step involves ATP-hydrolysis that energizes and rearranges the core complex making it competent for Ca^{2+}-induced fusion (17-21). Since the C-terminal domain of SNAP-25 binds tightly to VAMP during docking (20,73), it is conceivable that VAMP is a complementary binding partner for the peptide. How does ESUP-A binding to VAMP block exocytosis?. A plausible mechanism considers that ESUP-A competes with SNAP-25 for binding to VAMP and, thereby, prevents the formation of the critical SDS-resistant complex, comprising SNAP-25-VAMP-syntaxin (17-21,73,74). Absence of this ternary complex would hinder the association of SNAP and NSF proteins and the subsequent ATP-hydrolysis, therefore, preventing vesicle docking, priming and fusion. Two findings suggest that the peptide binds directly to VAMP and interrupts the subsequent chain of protein-protein interaction events that lead to vesicle fusion. First, ESUP-A promotes the accumulation of secretory vesicles near the active zone (Fig. 4). Second, the peptide arrests the ATP-dependent maturation of the secretory granules.

ESUP-A Mimics The Action Of Botxa On Exocytosis

As indicated in the scheme BoTxA and ESUP-A produce comparable effects on the Ca^{2+}-regulated fusion events that lead to transmitter release. Both BoTxA and ESUP-A inhibit the slow component of the Ca^{2+}-dependent exocytosis without affecting the fast component. Both attenuate to a similar extent the ATP primed exocytosis and not the ATP-independent exocytosis; and both increase the number of vesicles accumulated near the active zone. It appears, therefore, that BoTxA and ESUP-A block exocytosis in chromaffin cells by inhibiting the process of vesicle docking (38).

The finding that ESUPs are blockers of neurotransmitter release (37-39) suggests that BoTxs disable the fusion process with such efficacy by a synergistic action of cleaving the substrate molecules which interact through non-covalent interactions to assemble into a fusion complex, and of releasing peptide products which block by inhibiting vesicle docking. This implies that saturation with peptides designed to mimic putative sequences that bind to complementary partner sequences on interacting proteins, and combinations thereof, may abrogate vesicle fusion and transmitter release. The notion embodied in the ESUP activity suggests alternative pathways to regulate synaptic vesicle exocytosis, and provides novel pharmacological tools to unravel the molecular components and details of the secretory cascade. The fact that these synthetic peptides mimic the action of *Clostridial* neurotoxins provides clues to develop peptide-based agents that may have practical medical application as potential therapy in disorders associated with involuntary muscle spasms.

MODULATION OF CLOSTRIDIAL NEUROTOXIN ACTIVITY BY TYROSINE PHOSPHORYLATION

Phosphorylation of Clostridial Neurotoxins

Protein tyrosine phosphorylation is a prominent covalent modification of the dichain 150 kDa *Clostridial* neurotoxins. As shown in Fig. 5*a*, both the 50 kDa LC and 100 kDa HC of botulinum neurotoxin serotypes A, B and E, and the structurally homologous tetanus neurotoxin were found to be specifically phosphorylated by the tyrosine kinase Src. Incubation of the neurotoxins in presence of Src and [γ-^{32}P]-ATP for 60 min resulted in the conspicuous incorporation of ^{32}P on both the HC and the LC of BoTxA, BoTxE, BoTxB and TeTx. Immunoblotting with anti-phosphotyrosine specific mAbs displays the occurrence of phosphotyrosines according to the banding pattern which is characteristic of these neurotoxins (Fig. 5*b*). Tyrosine phosphorylation appears to be specific, as illustrated in Fig. 5*c;* BoTxA was not effectively phosphorylated by protein-serine/threonine kinases such as PKA whereas modest phosphorylation, especially of the HC, was obtained by PKC. The extent of tyrosine phosphorylation was time dependent, with an apparent half-maximum after ~15 min (Fig. 6*a*, 6*c*). At saturation, the stoichiometry of phosphorylation was ~1.0 mol ^{32}P/mol Tx chain for both the LC and the HC, suggesting the presence of a unique phosphorylation site. The reaction was reversible as demonstrated by dephosphorylation in presence of PTP-1B (Fig. 6*b*, 6*c*). Together, these results demonstrate that *Clostridial* neurotoxins can be heavily phosphorylated specifically at tyrosine residues (51).

Tyrosine Phosphorylation Augments The Protease Activity Of Clostridial Neurotoxins

Clostridial neurotoxins act as sequence specific endoproteases to cleave certain constituents of the synaptic vesicle docking/fusion complex (6-12). To assess the effect of tyrosine phosphorylation on proteolysis of its substrate the efficacy of BoTxA in cleaving *in vitro* translated SNAP-25 (51,75) was examined (Fig. 6*d,* 6*f*, Fig. 7). Neurotoxin activity was determined by a change in apparent mobility of the major product from 25 to 23 kDa (11,12). These assays revealed a marked increment in protease activity which was concurrent with the increase in the extent of tyrosine phosphorylation and, accordingly, that as BoTxA was dephosphorylated its activity was diminished (Fig. 6*c,e,f*). The extent of tyrosine phosphorylation of BoTxA, therefore, correlates with an increase in protease activity (51).

We next compared the protease activity of unphosphorylated (U) and phosphorylated (P) forms of BoTxA and BoTxE. In Fig 7*a*, the BoTxA concentration dependence for cleavage is shown in the left section of the gels (first five lanes, left to right) and the time dependence of proteolysis in the right section (last four lanes, left to right). Panels A and B show that, at 10 nM, phosphorylated neurotoxin led to virtually complete substrate cleavage, whereas at 50 nM unphosphorylated neurotoxin ≤50% of substrate remained uncleaved. Moreover, the time course of the assay shows that, at 10 nM, phosphorylated neurotoxin cleaved practically all SNAP-25 within 5 minutes of reaction, whereas the unphosphorylated neurotoxin required ≥30 min to achieve comparable proteolysis. Similar results were obtained for BoTxE (Fig. 7*a,* panels C and D). Compared to BoTxA which cleaves SNAP-25 at Gln197-Arg198 bond to release a nine aa fragment, BoTxE cuts between Arg180-Ile181 releasing a 26 aa fragment (9,12), which resulted in a greater separation of the bands corresponding to cleaved and uncleaved SNAP-25 substrate. Similar to BoTxA, tyrosine phosphorylation markedly increased the protease activity of BoTxE achieving maximal proteolysis rate at lower [BoTxE] and with shorter incubation times. These results show the striking augmentation of the catalytic activity of BoTxA and BoTxE that is produced by specific protein tyrosine phosphorylation (51).

Tyrosine Phosphorylation Increases The Thermal Stability Of Clostridial Neurotoxins

The potentiation of protease activity produced by protein tyrosine phosphorylation is accompanied by an increase in thermal stability of the neurotoxins (Fig. 7*b*). Incubation of phosphorylated (P) and unphosphorylated (U) forms of the neurotoxins at 22°C and 37°C prior to the addition of the SNAP-25 substrate showed that the proteolytic activity decayed substantially in a time- and temperature-dependent manner. Remarkably, phosphorylated neurotoxin exhibited a pronounced stabilization, evidenced by the delayed inactivation of its proteolytic activity at the temperatures studied. After exposure to 37°C for 10 h, phosphorylated neurotoxin exhibited ≥60% protease activity whereas unphosphorylated neurotoxin was virtually inactive in ~ 2 h. Protection of protease activity provides evidence of thermal stabilization consequent to the covalent modification of the toxin by tyrosine phosphorylation (51).

These results raised the intriguing question of whether tyrosine phosphorylation could restore the activity of thermally-inactivated neurotoxin. To examine this issue, BoTxA was first incubated at 37°C for 6 h to ensure ≥90% inactivation (Fig. 7*b*). Neurotoxin was then separated in two samples, one of which was phosphorylated by Src for 60 min at 30°C, prior to the assay of proteolytic activity. As shown in Fig. 7*c*, tyrosine phosphorylation reconstituted the protease activity of previously inactivated neurotoxin whereby phosphorylated toxin reached maximal activity at lower [BoTxA] and shorter reaction times than the unmodified neurotoxin. Tyrosine phosphorylation, therefore, appears to regenerate the catalytic activity of the LC, presumably by promoting the proper refolding and hence active conformation of the protease (51).

Tyrosine Phosphorylation Of Clostridial Neurotoxins Internalized Into Neurosecretory PC12 Cells

To investigate the biological significance of these *in vitro* modifications of BoTxs we examined whether the neurosecretory PC12 cells would effectively phosphorylate internalized BoTxA at tyrosine residues. PC12 cells express high levels of Src which can be exacerbated by exposure to NGF (76,77). PC12 cells were therefore incubated with 100 nM BoTxA for 12 h before lysis and cell extracts were probed with an antiphosphotyrosine mAb. In NGF-differentiated PC12 cells exposed to BoTxA, a faint band comigrating at the position expected for BoTxA LC was labeled with the antiphosphotyrosine mAb, suggesting that BoTxA LC is tyrosine-phosphorylated within these cells. PC12 cells exhibit Ca^{2+}-dependent neurotransmitter release (78); moreover, it is interesting that PYK2, a protein tyrosine kinase abundant in PC12 cells, is activated by stimuli that elevate the intracellular $[Ca^{2+}]$($[Ca^{2+}]_i$) (49), and Ca^{2+} influx mimics the action of NGF on neurite growth (46-48). To examine if induction of Ca^{2+} influx would enhance phosphorylation of internalized BoTxA, PC12 cells were incubated with 100 nM BoTxA, lysed, and tyrosine phosphorylated proteins immunoprecipitated with the antiphosphotyrosine mAb followed by SDS-PAGE. As shown in Fig. 8*a*, immunoblots probed with an anti-BoTxA LC mAb revealed a prominent band corresponding to the LC only in cells treated with BoTxA after depolarization with 75 mM KCl leading to the elevation of $[Ca^{2+}]_i$. Omission of Ca^{2+} markedly diminished the extent of LC tyrosine phosphorylation (Fig. 8*b*). Together, these results indicate that BoTxA internalized by NGF-differentiated PC12 cells undergoes strong phosphorylation by protein tyrosine kinases (51).

Modulation Of Neurotoxin Activity By Intracellular Signaling Cascades

These new findings that *Clostridial* neurotoxins are substrates of protein tyrosine kinases, and that tyrosine phosphorylation results in prominent augmentation of BoTx proteolytic activity and thermal stability, suggest that the phosphorylated form of these neurotoxins may be the physiologically active species within neurosecretory cells. Indeed, demonstration of intracellular tyrosine phosphorylation of BoTxA by selective stimulation of PC12 cells provides strong support to this idea. To our knowledge, the results show for the first time that a family of bacterial

neurotoxins is regulated by protein tyrosine phosphorylation. This previously unrecognized modification of BoTxA may therefore provide a mechanism to explain the long term paralytic effects exerted by these neurotoxins, from several days in cell culture up to several weeks even months in animals and humans and can account for documented discrepancies between *in vitro* frailty of these neurotoxins and the apparent *in vivo* stability as inferred from their long term effects (1-6, 44,45). These findings also raise the possibility that the role played by the tyrosine phosphorylation of BoTxA and E, which disable the vesicular fusion process required for neurotransmission, may be subject to regulation by intracellular signaling pathways that ultimately affect vesicular traffic. These cascades involve tyrosine kinases/phosphatases, G-proteins, phosphoinositides and calcium (46-49, 79-83). The "calcium-connection" is significant as it is known that tyrosine kinase activity is modulated by increases in $[Ca^{2+}]_i$ which may be evoked by extracellular stimuli and, notably, that tyrosine kinases such as Src and PYK2 are highly abundant in brain and neuroendocrine cells (4, 46-49). The potentiation of BoTxA and E protease activity by tyrosine phosphorylation suggests that a focus on intracellular modulation of tyrosine kinases and phosphatases as a new means of intervention in botulinum neurotoxicity deserves serious consideration (51).

IDENTIFICATION OF THE ION CHANNEL-FORMING MODULE IN BOTULINUM TOXIN A

Sequence Analysis

Amino acid sequence analysis suggests the occurrence of a potential transmembrane segment (TM) in BoTxA HC. This segment encompasses amino acids 659-681, with sequence GAVILLEFIPEIAIPVLGTFALV. Hydropathic power spectral analysis confirms the assignment and predicts an amphipathic α-helical structure (63,64). A peptide with a sequence corresponding to this segment, denoted as BoTxATM, was synthesized and purified by HPLC. Electrospray mass analysis of the HPLC peak (Fig. 9) shows three peaks. The principal peak with *m/z*=1199.0 corresponds to a material with a measured mass of 2396, the expected molecular mass [calculated average isotope composition of 2395.96 daltons], in accord with the anticipated amino acid composition of the peptide. The *m/z*= 1210.0 represents the same compound with Na^+ adsorbed whereas the peak with *m/z*= 1205.0 is an impurity (66).

Channel Formation By BoTxATM

A peptide with a sequence corresponding to the amphipathic segment of BoTxA HC forms ion channels in lipid bilayers (66).This is illustrated in Figure 10.

The most common pattern of channel occurrences is in the form of bursts of activity. Within these bursts of activity, the residence times of the channels in the open or closed states are not uniform, yet they present a consistent pattern with occurrences that are very short-lived (< 1 ms) and others which have residence times of several hundred ms. The most frequent events have a single channel conductance (γ) of 12 ± 1 pS and 6.5 ± 1 pS (n, number of experiments, = 17) in symmetric 0.5 M NaCl [Fig 10A, B], and 29 ± 2 pS and 9 ± 1 pS (n = 37) in 0.5 M KCl [Fig 10 C, D]. The current histograms identify the occurrence of two discrete states, closed and open, for these primary conductances. These are illustrated in Fig. 11A for the γ= 29 pS in KCl and in Fig. 11B for the γ= 12 pS in NaCl. Discrete openings with smaller or larger conductances are also discerned. Their occurrence is sporadic and the channel open times of the larger conductance events are significantly shorter than those of the primary conductances. The heterogeneity of conductance species observed with BoTxATM, both in amplitude and in the time that the channels remain open, is anticipated for an amphipathic peptide that self-assembles in the membrane to form non-covalent conductive oligomers of different sizes (66).

The BoTxATM channel is ohmic, as illustrated in Fig. 12. The slope conductance is 12 pS, which corresponds to the γ of the most frequent channel recorded in NaCl (66).

Sequence Specificity And Controls.

A peptide of the same amino acid composition as BoTxATM but with a computer-generated random sequence, predicted to retain a propensity for α-helix formation was synthesized. The sequence is EAVLLILIFPALGIPIGVTAFVE. This peptide interacts with bilayers, as manifested by stray fluctuations in membrane current; however, it does not form discrete conducting events (n = 4) (data not shown). These results support the specificity of the identified sequence as a candidate for the pore (66).

Comparison With Authentic Botx Channels And Inferences About Functional Role Of This Protein Module

All isoforms of BoTx form ion channels in lipid bilayers (52-54,60). TeTx forms cation-selective channels in lipid bilayers (52,58-61). For all these toxins, channel formation is more effective at acidic pH. The amino-terminal fragments of the heavy chains of the neurotoxins form channels which, at pH 7.0, exhibit heterogeneous conductances: For BoTxB, the most frequent openings exhibit $\gamma \simeq 15$ pS whereas for TeTx $\gamma = 45$ pS, in 1M KCl (52). At pH 4.0, the predominant single channel conductances were $\gamma = 20$ pS and $\gamma = 15$ pS, respectively (52). These latter values approximate those measured at neutral pH with the peptide mimics BoTxATM (66) and TeTx (63). This suggests that pH may be necessary to drive a conformational change in the holotoxin thereby exposing the transmembrane sequence, which then inserts into the bilayer core and eventually assembles into a conductive oligomer.

Concordant with expectations, the channel properties of BoTxATM approximate those of intact authentic toxin (52,53). BoTxATM is amphipathic, and when inserted into a membrane, presumably assembles into an oligomeric transmembrane structure. The tetrameric organization inferred from image reconstruction analysis (65) suggests that a channel structure may be modeled as a four-helix bundle. Conformational energy calculations indicate that the minimized four-helix bundle is compatible with the channels observed after reconstitution in bilayers (66). The occurrence of prolines at positions 10 and 15 introduces a pronounced kink on the helices and, therefore, an expansion of the pore diameter at this level. Transverse sections across the bundle indicate the occurrence of two discrete rings of carboxylates generating a considerable negative charge within the pore. Such rings may underlie the cation selectivity of the toxin channel. The hydrophilic residue T19 also faces the pore lumen and may contribute to the permeation properties of the channel. Hence, bundles of amphipathic α-helices fulfill the structural and energetic requirements to form the cation-selective pore identified in reconstitution studies of the intact toxins in lipid bilayers (52-54).

The toxin channel is conjectured to be involved in the translocation of the protein across the endocytic vesicle that exposes the LC protease to the cytosol. The dimensions of the channel, inferred from lipid bilayer measurements of single channel conductance and cut-off size of permeant ions, suggest that a pore diameter of ~8 Å would be compatible with the permeation pathway required for an extended peptide chain (52,54,60). Our findings support the notion that the HC may act as a channel through which the LC enters the cytosol (66). It will be interesting to explore if the BoTxATM channel is blocked by the LC or LC peptides, a finding that would lend credence to the notion that the channel activity is involved in LC translocation. The channel-forming sequence contained in the toxin HC is highly conserved in all BoTx isoforms and in the structurally homologous tetanus neurotoxin (63), suggesting a functional role for this conserved motif. The consensus sequence is: GAAILLEFIPELTIPVIGAFTIE (66). Identification of this functional module and the single channel assay of its activity provide opportunities for screening

and designing BoTxA channel blockers directed to abrogate the translocation of the BoTxA LC into the cytosol and, presumably, interfere with its cellular toxicity.

CONCLUSIONS

A most exciting outcome of this program is the ability to design peptides that selectively block neurotransmitter release. Indeed, the proteolytic peptide products of the BoTxA activity have proved to be instrumental in providing clues about the fusion process. These peptides are suitable mimics of the toxin itself, displaying effective inhibitory activity on transmitter release by disabling the fusion machinery. Peptides designed along these principles may find clinical application as BoTx substitutes in the treatment or management of disorders associated with involuntary muscle spasms. Alternatively, this approach may be conceived as a means to devise new methods for the treatment and medical management of BoTx casualties. The impact of this endeavor would be enormous if the design of synaptic vesicle-specific fusogenic peptides were practically realized into safe and well tolerated agents that would effectively restore neurotransmitter release and bypass the neuroparalytic toxic action of BoTxs.

A unique contribution of this program is the discovery of potentiation of BoTxA protease activity by tyrosine phosphorylation. This key finding underscores the requirement to screen for potential blockers using the pharmacologically relevant target, namely tyrosine phosphorylated toxin, presumably the biologically active form of the toxin within the cells. Thus, a focus on intracellular inhibition of tyrosine kinases and/or activation of tyrosine phosphatases as a parallel pathway for intervention in BoTxA toxicity deserves serious consideration.

A major aspect of this program was the identification of an ion channel-forming motif in BoTxA HC that may play a functional role in the ion channel-forming activity of intact BoTxA. These findings support the model of a bundle of four amphipathic α-helices as a plausible structural motif underlying the BoTxA channel. The ion channel activity of the HC may be abrogated by identifying effective open channel blockers. Assay of channel blocking activity is readily feasible using single channel recordings of the BoTxA HC reconstituted in lipid bilayers. This provides a sensitive assay to evaluate the concept that open channel blockers may be a single class of drugs effective against all BoTxs isoforms. The potency of such agents may, in principle, be augmented by combining active compounds against both the protease and channel activities of the toxin which are considered necessary for its neurotoxicity.

REFERENCES

1. Simpson, L.L. (1981) *Pharmacol. Rev.* **33,** 155-187.
2. Boroff, D.A., and DasGupta, B.R. (1971) in *Microbial Toxins (*Kadis, S., Monties, T.C.,and Ajl, S.J., eds) Vol 2A, pp 1-68, Academic Press, New York.
3. Jankovic, J. (1994) *Curr. Opin. Neurol.* **6,** 358-366.
4. Sudhof, T.C. (1995) *Nature* **375,** 645-653.
5. Scheller, R.H. (1995) *Neuron* **14,** 893-897.
6. Schiavo, G., Benfenati, F., Poulain, B., Rossetto, O., Polverino de Laureto, P., DasGupta, B.R., and Montecucco, C. (1992) *Nature* **359,** 832-835.
7. Schiavo, G., Rosetto, O., Santucci,. A, DasGupta, B.R., and Montecucco, C. (1992) *J. Biol. Chem.* **267,** 23479-23483.
8. Schiavo, G., Rosetto, O., Catsicas, S., Polverino de Laureto, P., DesGupta, B.R., Benfenati, F., and Montecucco, C. (1993) *J. Biol. Chem.* **268**, 23784-23787.
9. Binz, T., Blasi, J., Yamasaki, S., Baumeister, A., Link, E., Sudhof, T.C., Jahn, R., and Niemann, H. (1994) *J. Biol. Chem.* **269**, 1617-1620.
10. Hayashi, T., McMahon, H., Yamasaki, S., Binz, T., Hata, Y., Sudhof, T.C., and Niemann (1994) *EMBO J.* **13**, 5051-5061.
11. Schiavo, G., Santucci, A., DasGupta, B.R., Mehta, P.P., Jontes, J., Benfenati, F., Wilson, M.C., and Montecucco, C. (1993) *FEBS Lett.* **335**, 99-103.
12. Blasi, J. , Chapman, E.R., Link, E., Binz, T., Yamasaki, S., De Camilli, P., Sudhof, T.C., Niemann, H., and Jahn, R. (1993) *Nature* **365**, 160-163.
13. Montecucco, C., Papini, E. and Schiavo, G. (1994) *FEBS Lett* . **346**, 92-98
14. Hooper, N.M. (1994) *FEBS Lett.* **354**, 1-6.
15. Montecucco, C. and Schiavo, G (1995) *Q. Rev. Biophys.* **28**,423-472.
16. Matthews, G. (1996) *Annu. Rev. Neurosci.* **19**, 219-233.
17. Calakos, N. and Scheller, R.H. (1996) *Physiol. Rev.* **76**, 1-29.
18. Jahn, R. and Südhof, T.C. (1994) *Annu. Rev. Neurosci.* **17**, 219-246.
19. Zucker, R.S. (1996) *Neuron* **17**, 1049-1055.
20. O'Connor, V., Augustine, G.J., and Betz, H. (1994) *Cell* **76**, 785-787.
21. Schweizer, F.E., Betz, H., and Augustine, G.J. (1995) *Neuron* **14**, 689-696.
22. Bark, I.C. and Wilson, M.C. (1994) *Proc. Natl. Acad. Sci. USA* **91**, 4621-4624.
23. Rothmann, J.E. (1994) *Nature* **372**, 55-63.
24. Söllner, T., Whiteheart, S.W., Brunner, M., Erdjument-Bromage, H., Geromanos, S., Tempst, P. and Rothman, J.E. (1993) *Nature* **362**, 318-324.
25. Südhof, T.C., Baumert, M., Perin, M.S., and Jahn, R. (1989) *Neuron* **2**, 1475-1481.
26. Elferink, L.A., Trimble, W.S., and Scheller, R.H. (1989) *J. Biol. Chem.* **264**, 11061-11064.
27. Chapman, E.R., An, S., Barton, N., and Jahn, R. (1994) *J. Biol. Chem.* **269**, 27427-27432.
28. Otto, H., Hanson, P.I, Chapman, E.R., Blasi, J., and Jahn, R. (1995) *Biochem. Biophys. Res. Commun.* **212**, 945-952..
29. Bennett, M.K., Calakos, N., and Scheller, R.H. (1992) *Science* **257**, 255-259.
30. von Rüden, L., and Neher, E. (1993) *Science* **262**, 1061-1065.
31. Yamasaki, S., Baumeister, A., Binz, T., Blasi, J., Link, E., Cornille, F., Rogues, B., Fykse, E.M., Sudhof, T.C., Jahn, R., and Niemann, H. (1994) *J. Biol. Chem.* **269**, 12764-12772.
32. Yamasaki, S., Binz, T., Hayashi, T., Szabo, E., Yamasaki, N., Eklund, M., Jahn, R., and Niemann, H. (1994) *Biochem. Biophys. Res. Commun.* **200**, 829-835.
33. Pellizzari, R., Rossetto, O., Lozzi, L., Giovedi', S., Johnson, E., Shone, C.C., and Montecucco, C. (1996) *J. Biol. Chem.* **271**, 20353-20358.
34. Foran, P., Lawrence, G.W., Shone, C.C., Foster, K.A., and Dolly, J.O. (1996) *Biochemistry* **35**,2630-2636.
35. Schiavo, G., Shone, C.C., Bennett, M.K., Scheller, R.H., and Montecucco, C. (1995) *J. Biol. Chem* **270**, 10566-10570.

36. Williamson , L.C., Halpen, J.L., Montecucco, C., Brown, J.E., and Neale, E.A. (1996) *J. Biol. Chem.* **271**, 7694-7699.
37. Gutierrez, L.M., Canaves, J.M., Ferrer-Montiel, A.V., Reig, J.A., Montal, M., and Viniegra, S. (1995) *FEBS Lett.* **372**, 39-43.
38. Gutierrez, L.M., Viniegra, S., Rueda, J., Ferrer-Montiel, A.V., Canaves, J.M., and Montal, M (1997) *J. Biol. Chem.* **272**, 2634-2639.
39. Ferrer-Montiel, A.V., Oblatt-Montal, M., Canaves, J.M., Gutierrez, L.M., Nelson, R., Yamazaki, M. and Montal, M. (1997) *Biosci. Rev.* (in press).
40. DeBello, W. M., Betz, H., and Augustine, G.J. (1993) *Cell* **74**, 947-950.
41. Geppert, M., Goda, Y., Hammer, R.E., Li, C., Rosahl, T.W., Stevens, C.F. and Südhof, T.C. (1994) *Cell* **79**, 717-727.
42. DeBello, W.M., O'Connor, V., Dresbach, T., Whiteheart, S.W., S.W., Wang, S. S.-H., Scheweizer, F.E., Betz, H., Rothman, J.E., and Augustine, G.J. (1995) *Nature* **373**, 626-630.
43. Cornille, F., Deloye, F., Fournie-Zaluski, M.-C., Roques, B.P., and Poulain, B. (1995) *J. Biol. Chem.* **270**, 16826-16832.
44. Sellin, L.C., Thesleff, S., and DasGupta, B.R. (1983) *Acta Physiol. Scand.* **119,** 127-133.
45. Shone, C.C., and Melling, J. (1992) *Eur. J. Biochem.* **207,** 1009-1016.
46. Brugge, J.S., Cotton, P.C., Queral, A.E., Barrett, J.N., Nonner, D., and Keane, R.W. (1985) *Nature* **316,** 554-557.
47. Maher, P.A. (1988) *Proc. Natl. Acad. Sci. USA* **85,** 6788-6791.
48. Rusanescu, G., Qi, H., Thomas, S.H., Brugge, J.S., and Halegoua, S. (1995) *Neuron* **15,** 1415-1425.
49. Lev, S., Moreno, H., Martinez, R., Canoll, P., Peles, E., Musacchio, J.M., Plowman, G.D., Rudy, B., and Schlessinger, J. (1995) *Nature* **376,** 737-745.
50. Sathyamoorthy, V., and DasGupta, B.R. (1985) *J. Biol. Chem.* **260,** 10461-10466.
51. Ferrer-Montiel, A.V., Canaves, J.M., DasGupta, B.R., Wilson, M.C., and Montal, M. (1996) *J. Biol. Chem.* **271**, 18322-18325.
52. Hoch, D.H., Romero-Mira, M., Erlich,B., Finkelstein, A., DasGupta, B.R., and Simpson, L.L. (1985) *Proc. Natl. Acad. Sci. USA* **82**, 1692-1696.
53. Donovan, J.J. and Middlebrook, J.L. (1986) *Biochemistry* **25**, 2872-2876.
54. Blaustein, R.O., Germann, W.J., Finkelstein, A., DasGupta, B.R. (1987) *FEBS Lett* . **226**, 115-120.
55. Boquet, P., Silverman, M.S., Pappenheimer, A.M.Jr, Vernon, W.B. (1976) *Proc. Natl. Acad. Sci. USA* **73**, 4449-4453.
56. Boquet, P., Duflot, E. (1982) *Proc. Natl. Acad .Sci. USA* **79**, 7614-7618.
57. Boquet, P., Duflot, E. and Hauttecoeur, B. (1984) *Eur. J. Biochem* . **144**, 339-344.
58. Borochov-Neori, H., Yavin ,E. and Montal, M. (1984) *Biophys. J.* **45**,83-85.
59. Gambale, F. and Montal, M. (1988) *Biophys. J.* **53**, 771-783.
60. Finkelstein, A.(1990) *J. Physiologie* **84**,188-190.
61. Rauch, G., Gambale, F. and Montal, M. (1990) *Eur. J. Biophys.* **18**,79-83.
62. Schmid, A., Benz, R., Just, I. and Aktories, K. (1994) *J. Biol. Chem* . **269**,16706-16711.
63. Montal, M.S., Blewitt, R., Tomich, J.M. and Montal, M. (1992) *FEBS Lett.* **313** 12-18.
64. Lebeda, F.J., Hack, D.C. and Gentry, M.K. (1994) In: Jankovic, J., Hallett, M., eds. *Therapy with Botulinum Toxin.* New York:Marcel Dekker. pp 51-61.
65. Schmid, M.F., Robinson, T.P. and DasGupta, B.R. (1993) *Nature* **364**,827-830.
66. Oblatt-Montal, M., Yamazaki, M., Nelson, R. and Montal, M. (1995) *Protein Sci.* **4**,1490-1497.
67. Hay, J.C. and Martin, T.F.J. (1992) *J. Cell Biol.* **119**, 139-151,
68. Bittner, M.A. and Holz, R.W. (1992) *J. Biol. Chem.* **267**, 16219-16225.
69. Parsons, T.D., Coorssen, J.R., Horstmann, H., and Almers, W. (1995) *Neuron* **15**, 1085-1096.
70. Bittner, M.A. and Holz, R.W. (1992) *J. Biol. Chem.* **267**, 16226-16229.
71. Lawrence, G., Weller, U, and Dolly, J.O. (1994) *Eur. J. Biochem.* **222**, 325-333.

72. Hunt, J.M., Bommert, K., Charlton, M.P., Kistner, A., Habermann, E., Augustine, G.J., and Betz, H. (1994) *Neuron* **12**, 1269-1279.
73. Hayashi, T., Yamasaki, S., Nauenburg, S., Binz, T., and Niemann, H. (1995) *EMBO J.* **14**, 2317-2325.
74. Calakos, N., and Scheller, R.H. (1994) *J. Biol. Chem.* **269**, 24534-24537.
75. Oyler, G.A., Higgins, G.A., Hart, R.A., Battenberg, E., Billingsley, M., Bloom, F.E., and Wilson, M.C. (1989) *J. Cell Biol.* **109**, 3039-3052.
76. Kremer, N.E., D'Arcangelo, G., Thomas, S.M., DeMarco, M., and Brugge, J.S. (1991) *J. Cell Biol.* **115,** 809-819.
77. Green, L.A., Aletta, J.M., Rukenstein, A., and Green, S.H. (1987) *Methods Enzymol.* **147,** 207-216.
78. Banerjee, A., Martin, T.F.J., and DasGupta, B.R. (1993) *Neurosci. Lett.* **164,** 93-96.
79. Liscovitch, M., and Cantley, L.C. (1995) *Cell* **81,** 659-662.
80. Clapham, D.E. (1995) *Cell* **80,** 259-268.
81. Heidelberger, R., Heinemann, C., Neher, E., and Matthews, G. (1994) *Nature* **371,** 513-515.
82. Levitzki, A., and Gazit, A. (1995) *Science* **267,** 1782-1787.
83. McPherson, P.S., Garcia, E.P., Slepnev,.V.I., David, C., Zhang, X., Grabs, D., Sossin, W.S., Bauerfeind, R., Nemoto, Y., and De Camilli, P. (1996) *Nature* **379,** 353-357.

*The abbreviations used are: BoTx, botulinum neurotoxin; TeTx, tetanus neurotoxin; HC, heavy chain; LC, light chain; DTT, dithiothreitol; PAGE, polyacrylamide gel electrophoresis; NGF, nerve growth factor; RIPA, radioimmunoprecipitation assay; SNAP-25, synaptosomal associated protein of 25 kDa; PTP-1B, protein-tyrosine phosphatase 1B; mAb, monoclonal antibody. ESUP, excitation-secretion uncoupling peptide; VAMP, vesicle associated membrane protein; NSF, N-ethylmaleimide-sensitive fusion protein; SNAP, soluble NSF attachment protein; SNARE, SNAP receptor; v-SNARE, vesicle SNARE; t-SNARE, target-SNARE; POPE/POPC 1-palmitoyl-2-oleoyl-*sn*-glycero-3-phosphoethanolamine (POPE) and 1-palmitoyl-2-oleoyl-*sn*-glycero-3-phosphocholine (POPC); TFE, trifluoroethanol; γ, single channel conductance; τ_o and τ_c, channel open and closed lifetimes.

FIGURES

Fig. 1. **A synthetic peptide representing the C-terminal sequence of SNAP-25 inhibits calcium-regulated exocytosis from permeabilized chromaffin cells.** Digitonin permeabilization lasted 5 min and radiolabeled noradrenaline secretion was evoked in the absence (5 mM EGTA) or presence of calcium. (A) Inhibition of exocytosis is sequence-specific. Shown is the effect on the basal and calcium-stimulated release of 100 μM of SNAP-25 (187-206)[SNKTRIDEANQRATKMLGSG], SNAP-25(195-201)[ANQRATK], SNAP-25(187-206)RD [TDSSGREMIKANKLANGTR], and SNAP-25(49-59)[MLDEQGEQLER]. (B) Dose-dependent inhibition of calcium-evoked secretion by SNAP-25(187-206). Net release is expressed. Data are mean ± SEM from 4 different experiments performed in triplicate. Statistical significance was assessed using the Student's *t*-test. $^*P < 0.01$ as compared with control in the absence of peptide.

Fig. 2. **ESUP-A blocks catecholamine secretion in permeabilized chromaffin cells evoked by the second of two consecutive Ca^{2+} pulses.** Secretion was elicited by 10 μM of free Ca^{2+} or in basal media (5 mM EGTA) for 2 min (1st pulse). Media were collected and cells were incubated for 5 min in Ca^{2+}-free buffer. Thereafter, a 10 min Ca^{2+} stimulation was applied (2nd pulse). Three conditions were assayed: Control; cells incubated with 100 μM ESUP-A (SNKTRIDEANQRATKMLGSG); and cells exposed to 100 μM ESUP-A^{RDM}, a 20-mer peptide with the same amino acid composition of ESUP-A but random sequence (TDSSGREMIKANKQLANGTR). The CPM released from control cells under basal conditions were ~4,000, and increased to ~13,000 after stimulation with 10 mM Ca^{2+}. The total number of counts obtained from detergent-permeabilized cells was ~130,000. Thus, the normalized basal and the Ca^{2+}-evoked release represent the 3.5% and ~10% of the total secretion, respectively. Data are given as mean ± SEM with n (number of experiments performed in triplicate) = 4.

Fig. 3. **ESUP-A affects the ATP-dependent step of the exocytotic process.** Ca^{2+}-evoked catecholamine secretion was elicited in presence (*left*) or absence (*right*) of 2 mM Mg-ATP at 37 °C. Three conditions were assayed: Control; 100 μM ESUP-A; and 100 μM ESUP-A^{RDM}. Catecholamine secretion was triggered with 10 μM Ca^{2+} for 10 min. Basal secretion was evoked with 5 mM EGTA. Net release denotes the release in excess of that obtained under basal conditions, as indicated in Fig. 2. Data are given as mean ± SEM with n=4, (experiments performed in triplicate). Other conditions were the same as described in the legend to Fig. 2.

Fig. 4. **ESUP-A induces changes in chromaffin granule distribution after Ca^{2+} stimulation of digitonin-permeabilized cells.** Cells were permeabilized as described in presence or absence of peptide. Secretion was triggered with 10 μM Ca^{2+} for 10 min. Thereafter, cells were collected by low speed centrifugation (1000xg, 2 min), fixed and processed for electron microscopy. (**A**) Photomicrographs of cells incubated in a 5 mM EGTA medium without added Ca^{2+} (Unstimulated). (**B**) Cells stimulated with 10 μM of free Ca^{2+}(Ca^{2+}-stimulated). (**C**) Ca^{2+}-stimulated cells in the presence of 100 μM of ESUP-A. (**D**) Ca^{2+}-stimulated cells treated with BoTxA. BoTxA (100 nM) inhibited ~60% of Ca^{2+}-induced neurotransmitter release. N denotes the cell nucleus. Magnification is 4,000-fold for (A) and 6,000-fold for (B, C, and D).

Fig. 5. **Tyrosine phosphorylation of *Clostridial* neurotoxins.** *a.* Src phosphorylates the HC and LC of BoTxA, BoTxB, BoTxE and TeTx. The autoradiograms display incorporation of ^{32}P into both LC (M_r ~50,000) and HC (M_r ~100,000). Toxins protein concentration was 250 nM; Src (3 Units) was incubated with toxins for 60 min at 30 °C. *b.* Immunoblot of a gel as that shown in *a* probed with an antiphosphotyrosine mAb (anti P-Tyr). *c.* BoTxA was strongly phosphorylated by Src, but not by PKA or PKC; PKC produced weak phosphorylation of the HC. Autoradiograms display ^{32}P incorporation into protein.

Fig. 6. **Kinetics of BoTxA phosphorylation and dephosphorylation by Src, and of the augmentation of BoTxA protease activity by protein tyrosine phosphorylation.** *a.* Extent of ^{32}P incorporation into BoTxA HC and LC as function of incubation time in presence of Src. BoTxA was incubated with Src (3 Units) at 30 °C for the indicated time periods, as described in Fig. 5. The middle band (M_r ~55,000) corresponds to autophosphorylated Src. *b.* Tyrosine-phosphorylated BoTxA is enzymatically dephosphorylated by PTP-1B. Tyrosine-phosphorylated BoTxA was incubated with PTP-1B for the indicated time periods. Controls include omission of PTP-1B or its inhibition by 200 mM Na orthovanadate (VO_4) (last lane). *c.* The extent of phosphorylation, 0-120 min (l) and dephosphorylation, 120-240 min (m) were quantified using an image analyzer; dashed lines are controls. *d.* Tyrosine phosphorylation of BoTxA is accompanied by augmentation of protease activity. Fluorograms display the mobility change of *in vitro* translated SNAP-25 due to proteolysis by BoTxA as function of phosphorylation time by Src; u=uncut and c=cleaved. First and last lanes show controls in which Src and/or BoTxA, respectively, were omitted. *e.* Dephosphorylation of BoTxA reduces its protease activity. Last lane shows the control in presence of 200 mM VO_4. *f.* Extent of proteolysis of SNAP-25 as function of phosphorylation of BoTxA by Src, 0-90 min (l) and dephosphorylation by PTP-1B, 90-210 min (m), quantified by image analysis as in *c*; dashed lines are controls denoting omission of BoTxA (l) or presence of VO_4 (m). Cleavage reaction time was 5 min for *d* and 15 min for *e*. Toxin concentration was 10 nM. Control samples include omission of kinases and for Src, in addition, preincubation with peptide A.

Fig. 7. **Augmentation of BoTx protease activity by protein tyrosine phosphorylation is accompanied by increased thermal stability.** *a.* A. Cleavage of SNAP-25 translated *in vitro* by unphosphorylated BoTxA (U) or tyrosine phosphorylated BoTxA (P) as function of [BoTxA] or incubation time at a fixed [BoTxA] (10 nM). B. Extent of SNAP-25 cleavage as function of [BoTxA] and incubation time quantified by image analysis of the fluorograms shown. C. Tyrosine phosphorylation of BoTxE increases its protease activity. Comparison of the cleavage of SNAP-25 by unphosphorylated BoTxE (U) or tyrosine phosphorylated BoTxE (P) as function of [BoTxE] or incubation time at a fixed [BoTxE] (10 nM). D. Extent of SNAP-25 cleavage as function of [BoTxE] or incubation time quantified by image analysis of the fluorograms shown. *b.* Increased thermal stability of BoTxA by tyrosine phosphorylation. Phosphorylated and unphosphorylated neurotoxins were incubated at either 22 °C or 37 °C for the indicated times and, thereafter, assayed for proteolytic cleavage of *in vitro* translated SNAP-25 at a fixed [BoTxA] (20 nM) for 15 min at 30 °C. Fluorograms were quantified as described in Fig. 6; phosphorylated (❑,○) and unphosphorylated (■,●) BoTxA. *c.* Tyrosine phosphorylation stabilizes the protease activity. BoTxA was incubated at 37 °C for 6 h, phosphorylated by Src for 60 min at 30 °C and assayed (■); non-phosphorylated samples (●) were equivalent but Src was omitted. Other conditions as described for Fig. 6.

Fig. 8. **Intracellular tyrosine phosphorylation of BoTxA LC in NGF-differentiated PC12 cells.** *a.* Cell extracts probed with an anti-BoTxA LC mAb (*top*), an anti-SNAP25 mAb (*middle*), and immunoprecipitates of tyrosine phosphorylated proteins (*bottom*) from NGF-differentiated PC12 cells treated with 100 nM BoTxA that were subjected to the following conditions: incubation with 75 mM KCl, in presence (1.8 mM $CaCl_2$) or absence (3 mM EGTA) of extracellular Ca^{2+}-for 5 min at 37 °C. The immunoprecipitates were washed, analyzed by 10% SDS-PAGE under non-reducing conditions and immunoblotted with a mAb against the N-terminal half of BoTxA LC (mAb#9). Immunoblotting with an anti-BoTxA HC mAb#6 produced no detectable signal. Whole cell extracts and immunoprecipitates were analyzed in 12% SDS-PAGE gels under reducing and non-reducing conditions, respectively. The diffuse bands appearing on the anti-LC blot of cell extracts (*top*) above the sharp bands corresponding to the BoTxA LC arise from background immunoreactivity against the second Ab (antimouse serum). The diffuse band appearing on the anti-LC blot of the IP (*bottom*) in absence of BoTxA corresponds to the heavy chain of the immunoglobulin with a M_r of 50,000 which is in the same range as that of LC. *b.* Data

of three different experiments such as that shown in *a* were quantified by image analysis and plotted in arbitrary units ± SEM. Note the sharp enhancement of LC tyrosine phosphorylation only in cells treated with BoTxA after depolarization with KCl in the presence of calcium.

Fig. 9. **Mass spectrum of the purified BoTxATM synthetic peptide**. *m/z* is the mass-to-charge ratio.

Fig. 10. **Single-channel currents from POPE/POPC bilayers containing the BoTxATM peptide**. Currents were recorded at V= 100 mV in symmetric 0.5 M NaCl (A,B) or KCl (C,D), 1 mM $CaCl_2$, 5 mM Hepes pH 7.4. Segments of a continuous record are displayed to illustrate the occurrence of the 12 pS channel (A), the 6.5 pS channel (B) in NaCl, and the 29 pS channel (C) and 9 pS channel (D) in KCl.

Fig. 11. **Current histograms.** Current histograms for the primary conductances, generated from continuous segments of records lasting several minutes, are displayed in (A) for KCl and in (B) for NaCl; CLOSED and OPEN denote closed and open states. The probability of the channel being open, P_o, or closed, P_c, is calculated from the area under the corresponding Gaussian curve. In NaCl, P_o = 0.43; in KCl, P_o = 0.77. The single-channel current is calculated as the difference between the peaks associated with the closed and open states. The corresponding values for single channel conductances are 29 pS (KCl) and 12 pS (NaCl). Records filtered at 1 kHz.

Fig. 12. **Current-voltage (*I-V*) characteristics of the single-channel events of BoTxATM channel in symmetric 0.5 M NaCl.** The single-channel *I-V* is ohmic with a slope conductance of 12 pS for the most frequent event. Currents reported as mean values ± S.D.; n=3.

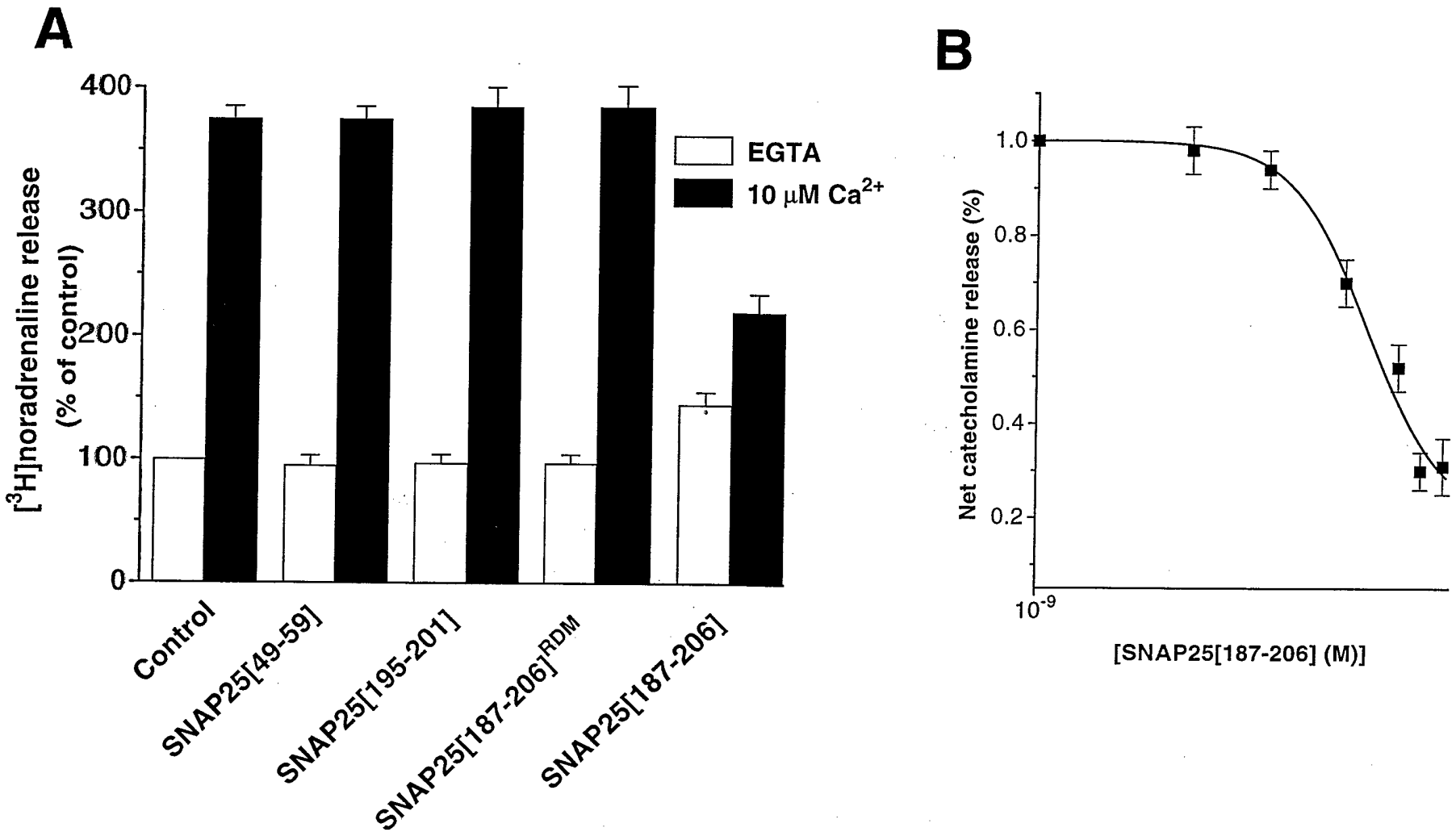
A
400
300
200
100
0
[3H]noradrenaline release (% of control)
EGTA
10 μM Ca2+
Control
SNAP25[49-59]
SNAP25[195-201]
SNAP25[187-206]RDM
SNAP25[187-206]
B
1.0
0.8
0.6
0.4
0.2
10-9
Net catecholamine release (%)
[SNAP25[187-206] (M)]

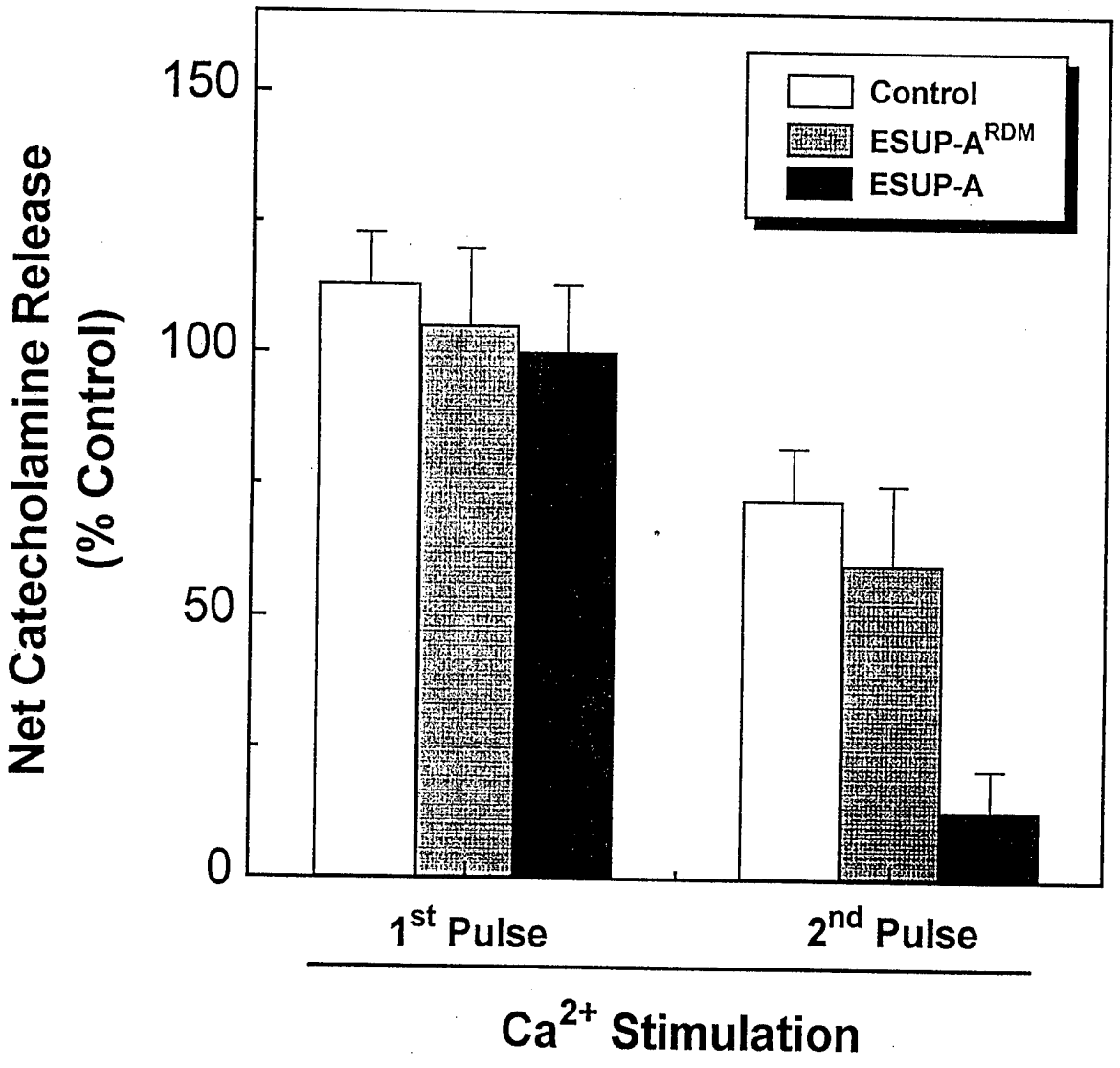
Net Catecholamine Release
(% Control)
150
100
50
0
Control
ESUP-A^RDM
ESUP-A
1st Pulse
2nd Pulse
Ca2+ Stimulation

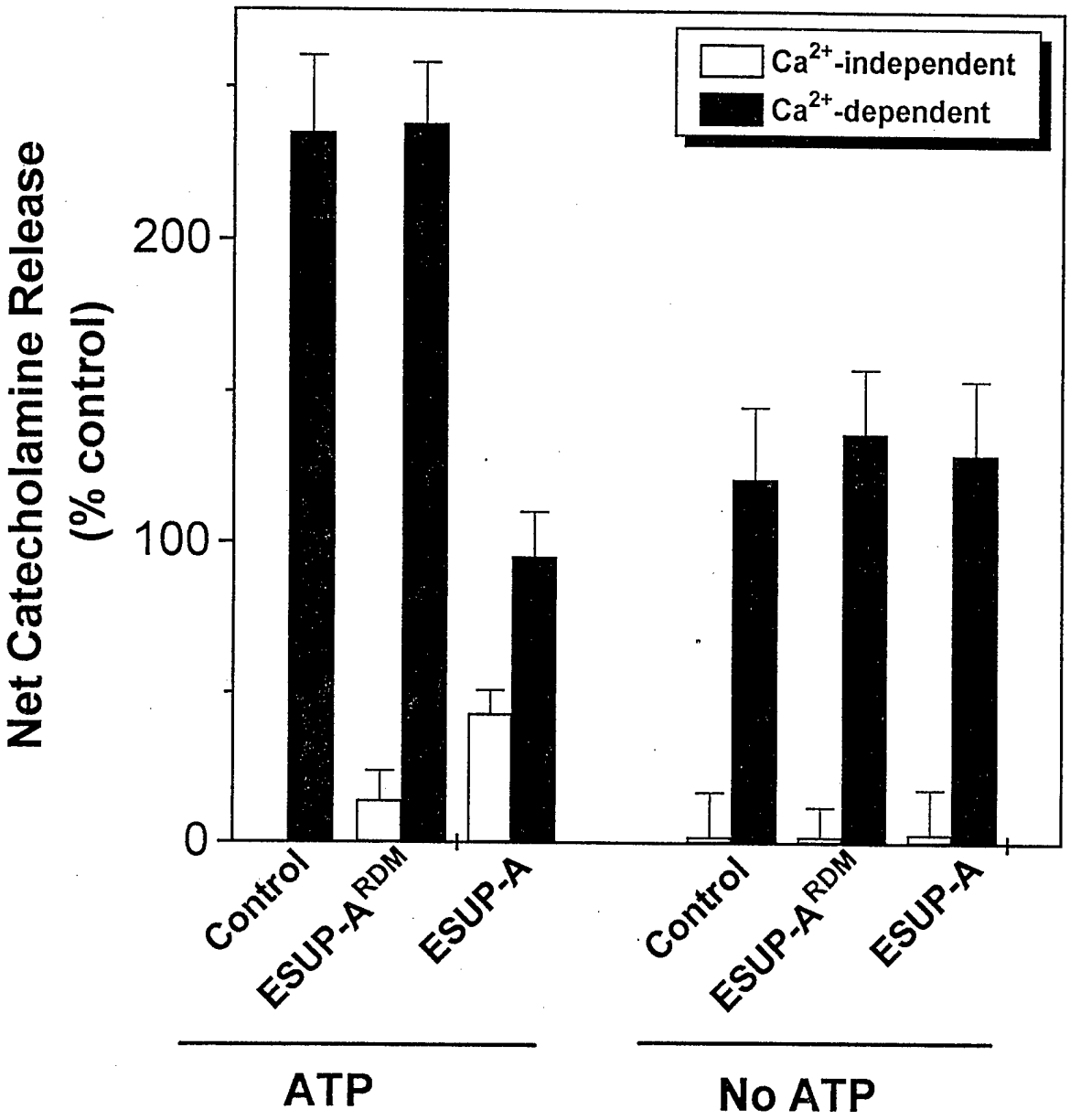
Net Catecholamine Release
(% control)
200
100
0
Ca2+-independent
Ca2+-dependent
Control
ESUP-ARDM
ESUP-A
Control
ESUP-ARDM
ESUP-A
ATP
No ATP

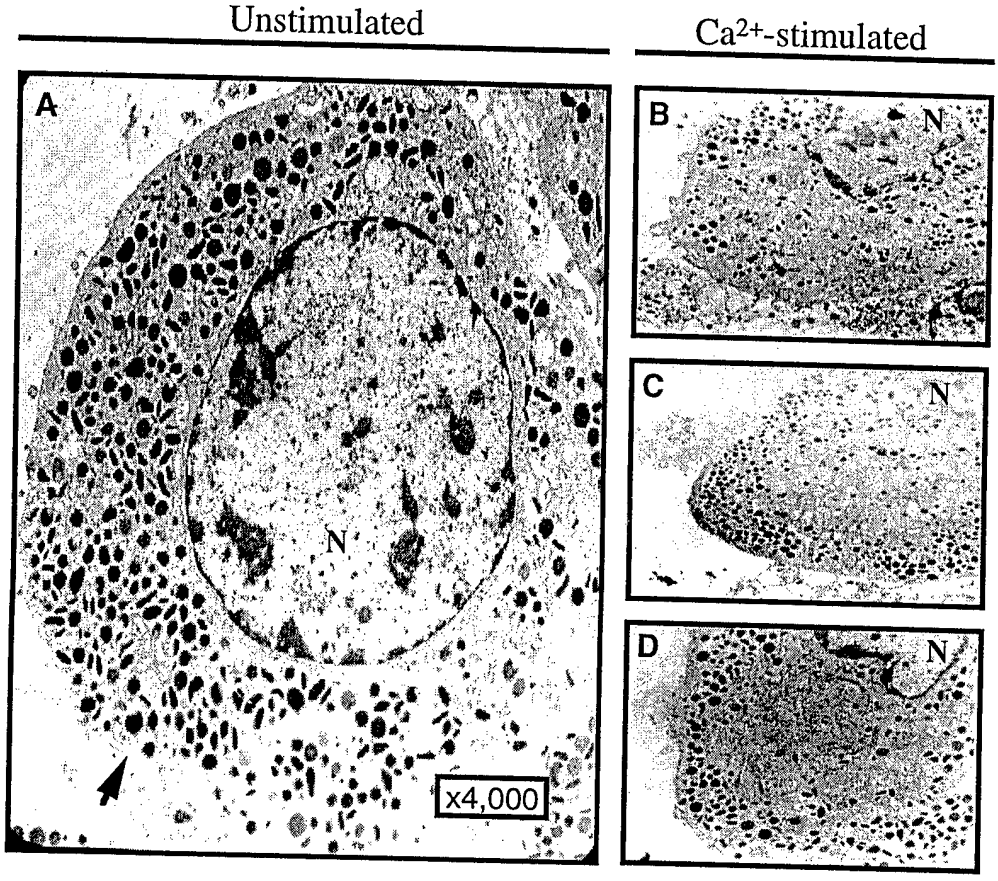
Unstimulated
Ca2+-stimulated
A
N
x4,000
B
N
C
N
D
N

a
32P
HC
LC
BoTxA
BoTxE
BoTxB
TeTx
b
Anti P-Tyr
BoTxA
BoTxB
BoTxE
TeTx
c
32P
100kD
50kD
BoTxA PKA Src PKC

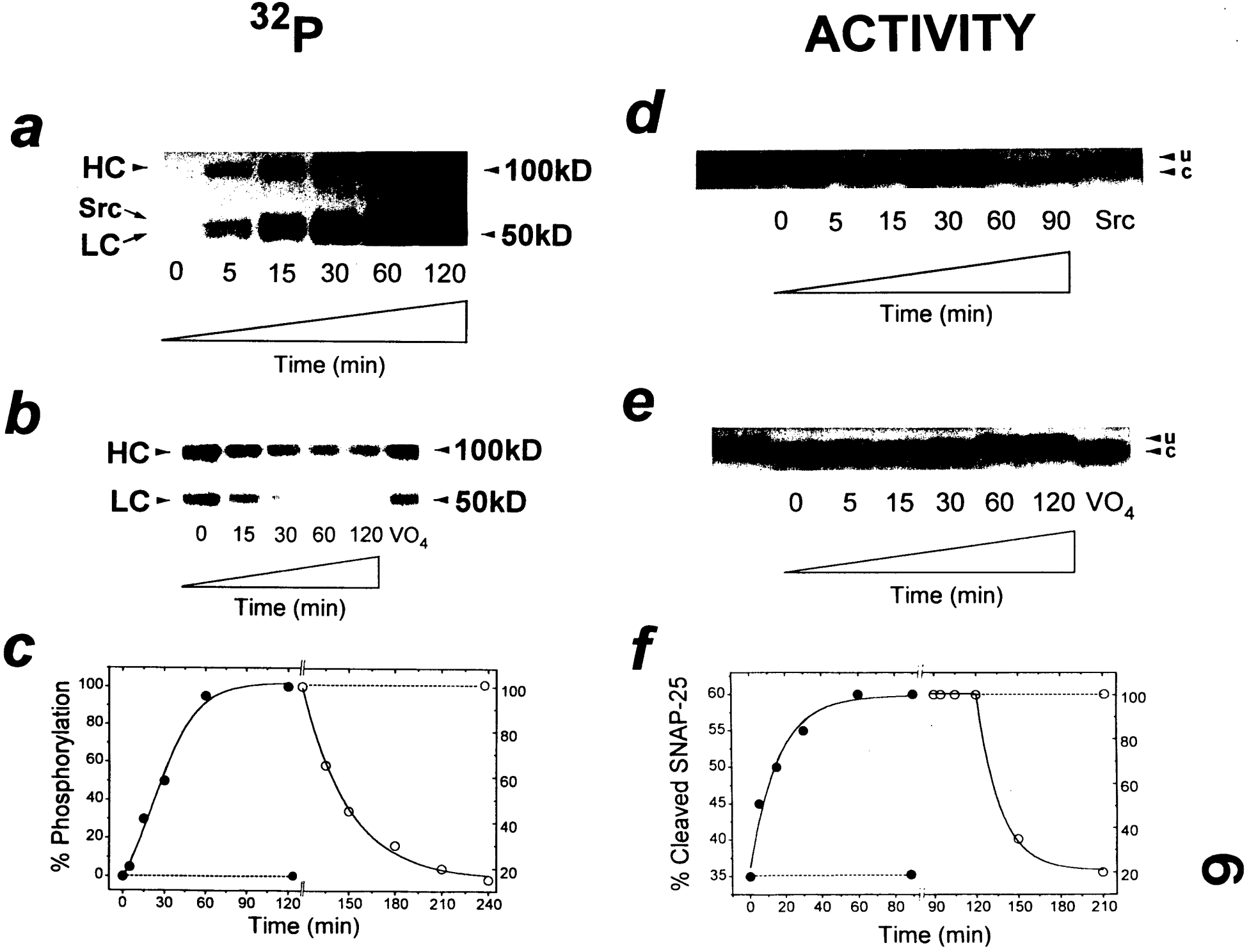
32P
ACTIVITY
a
HC
Src
LC
100kD
50kD
0 5 15 30 60 120
Time (min)
b
HC
LC
100kD
50kD
0 15 30 60 120 VO4
Time (min)
c
% Phosphorylation
Time (min)
d
u
c
0 5 15 30 60 90 Src
Time (min)
e
u
c
0 5 15 30 60 120 VO4
Time (min)
f
% Cleaved SNAP-25
Time (min)

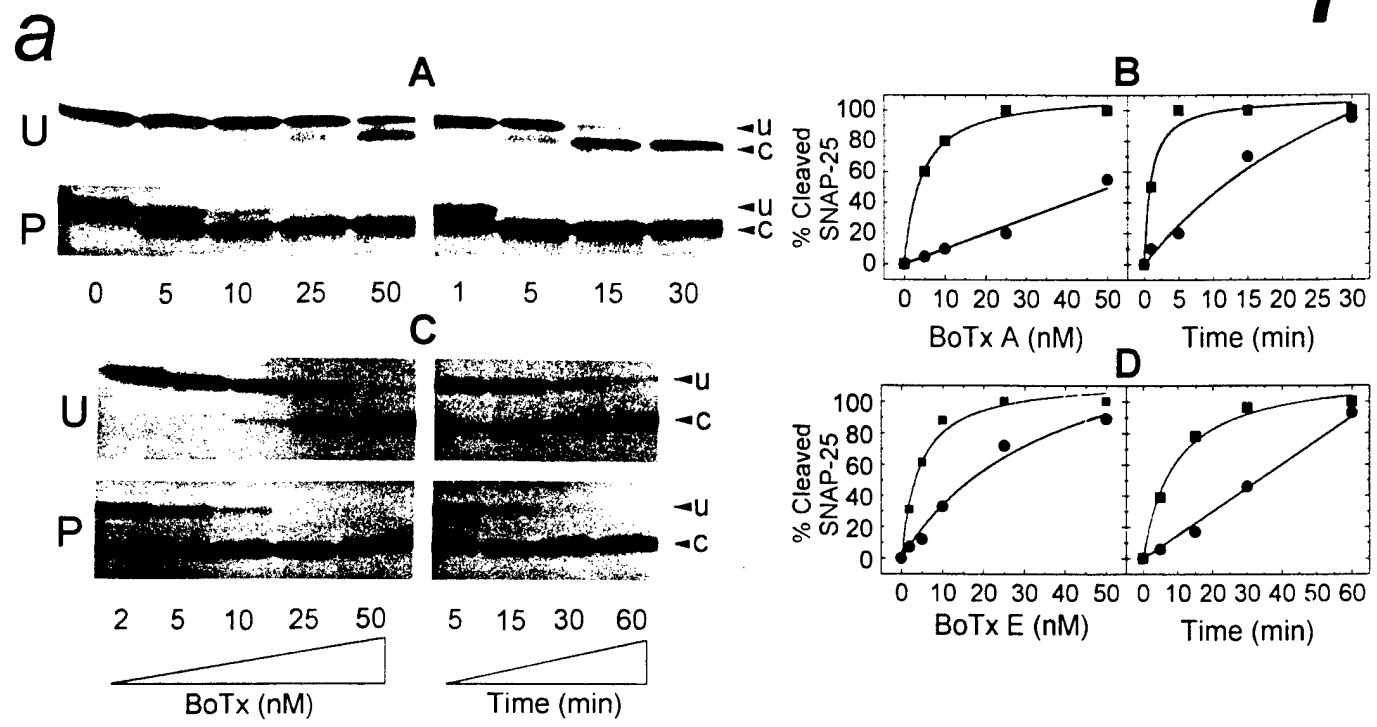
a
A
U
P
u
c
0 5 10 25 50 1 5 15 30
C
2 5 10 25 50
5 15 30 60
BoTx (nM)
Time (min)
B
% Cleaved SNAP-25
0 10 20 30 40 50
BoTx A (nM)
0 5 10 15 20 25 30
Time (min)
D
0 10 20 30 40 50
BoTx E (nM)
0 10 20 30 40 50 60
Time (min)

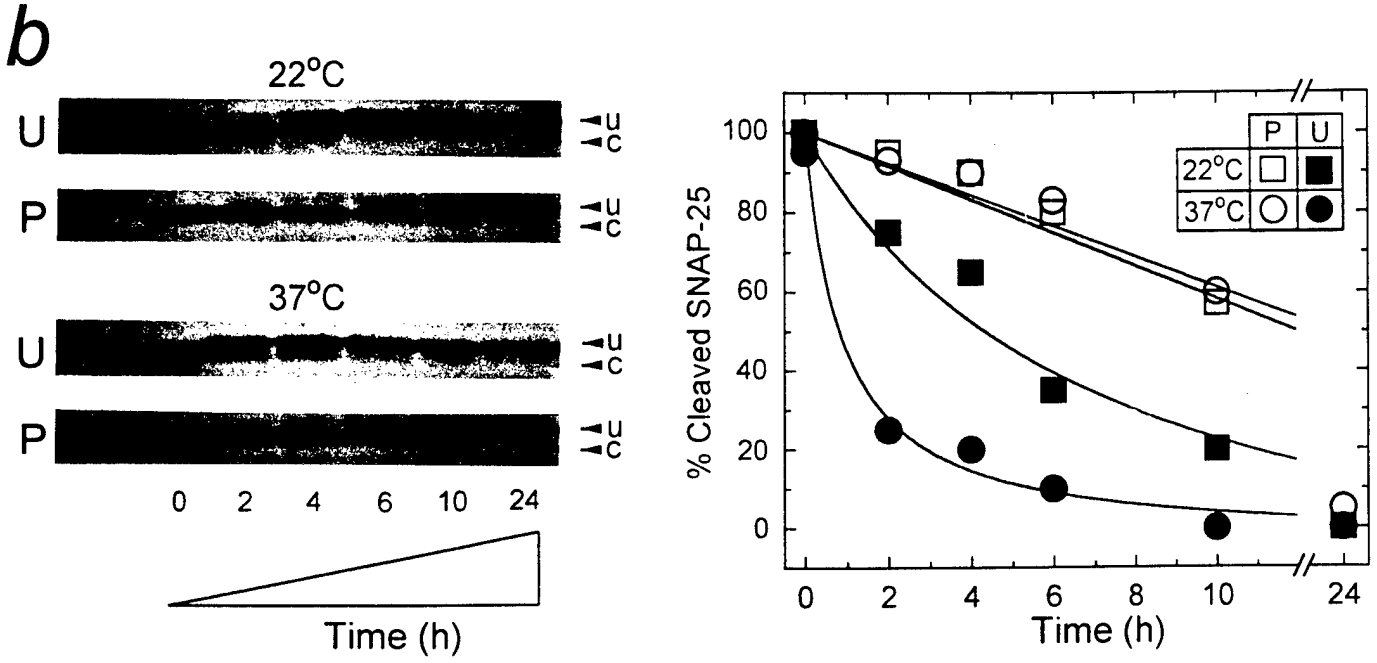
b
22°C
37°C
U
P
0 2 4 6 10 24
Time (h)
% Cleaved SNAP-25
P U
22°C
37°C
0 2 4 6 8 10 24
Time (h)

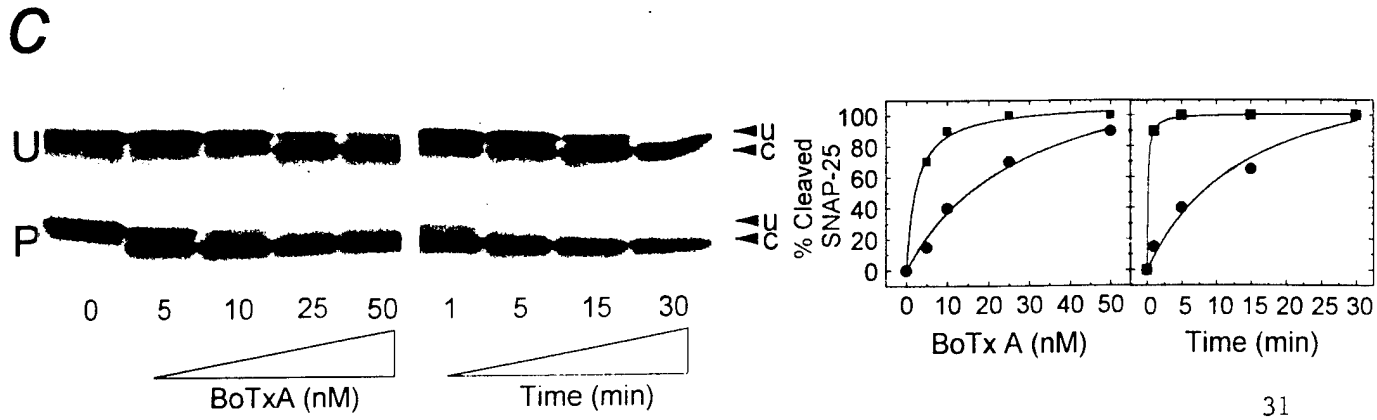
c
U
P
0 5 10 25 50 1 5 15 30
BoTxA (nM)
Time (min)
% Cleaved SNAP-25
0 10 20 30 40 50
BoTx A (nM)
0 5 10 15 20 25 30
Time (min)

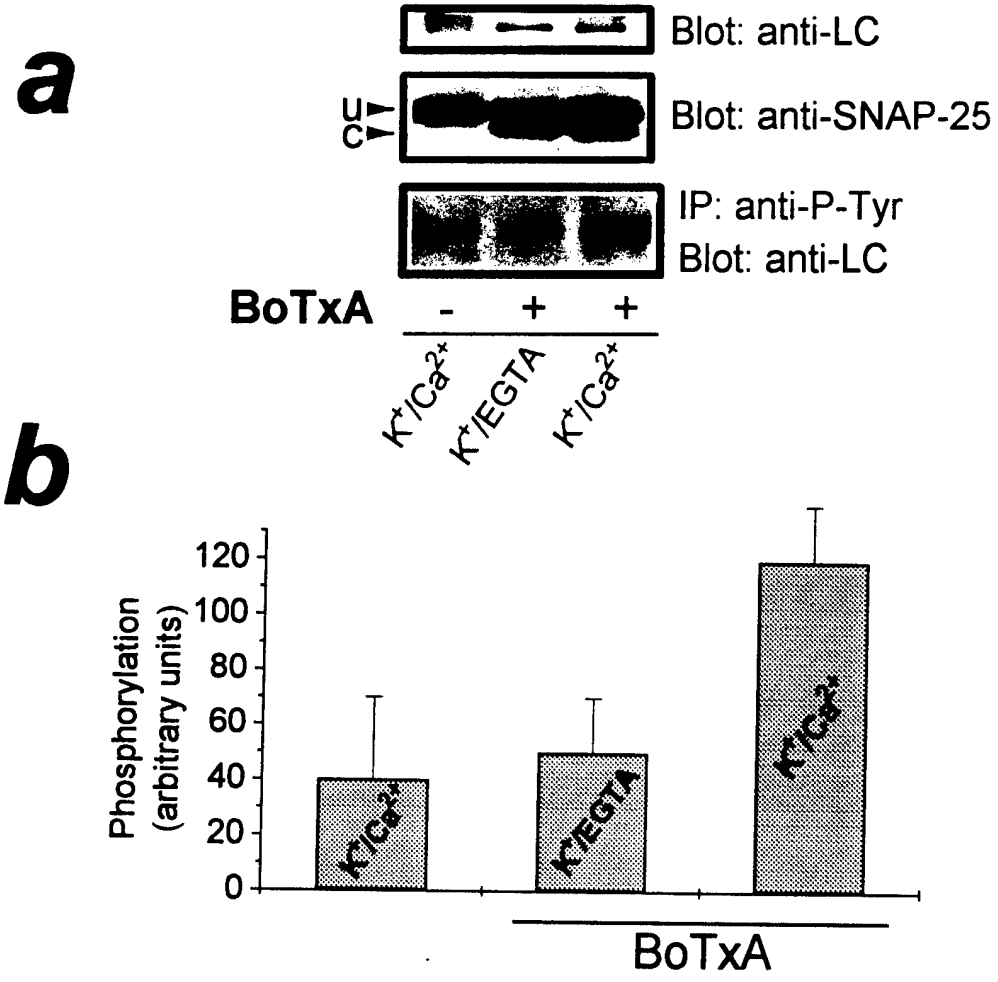
a
Blot: anti-LC
U
C
Blot: anti-SNAP-25
IP: anti-P-Tyr
Blot: anti-LC
BoTxA - + +
K+/Ca2+
K+/EGTA
K+/Ca2+
b
Phosphorylation (arbitrary units)
120
100
80
60
40
20
0
K+/Ca2+
K+/EGTA
K+/Ca2+
BoTxA

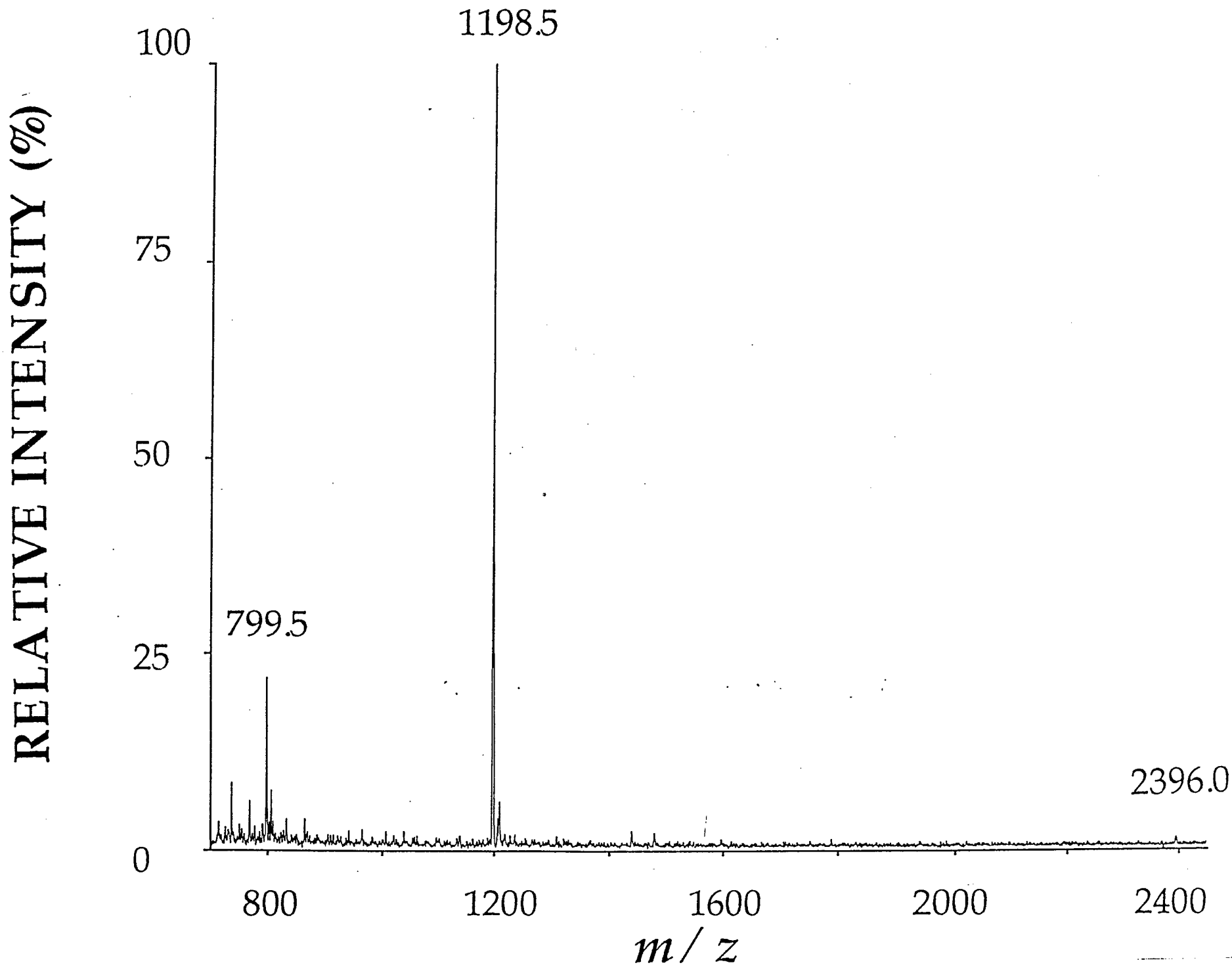
1198.5
100
75
50
799.5
25
2396.0
0
800
1200
1600
2000
2400
RELATIVE INTENSITY (%)
m / z

6

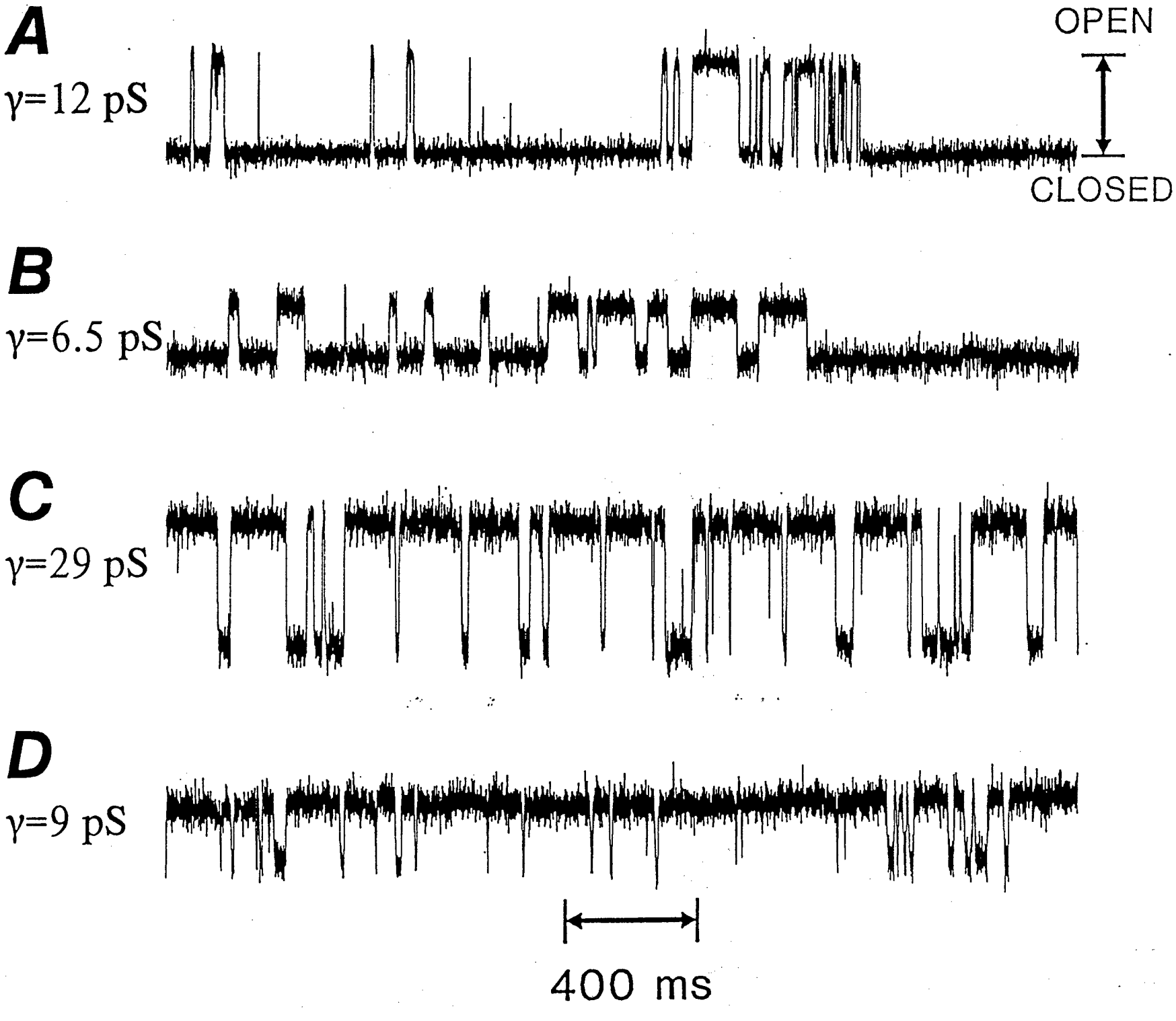

10

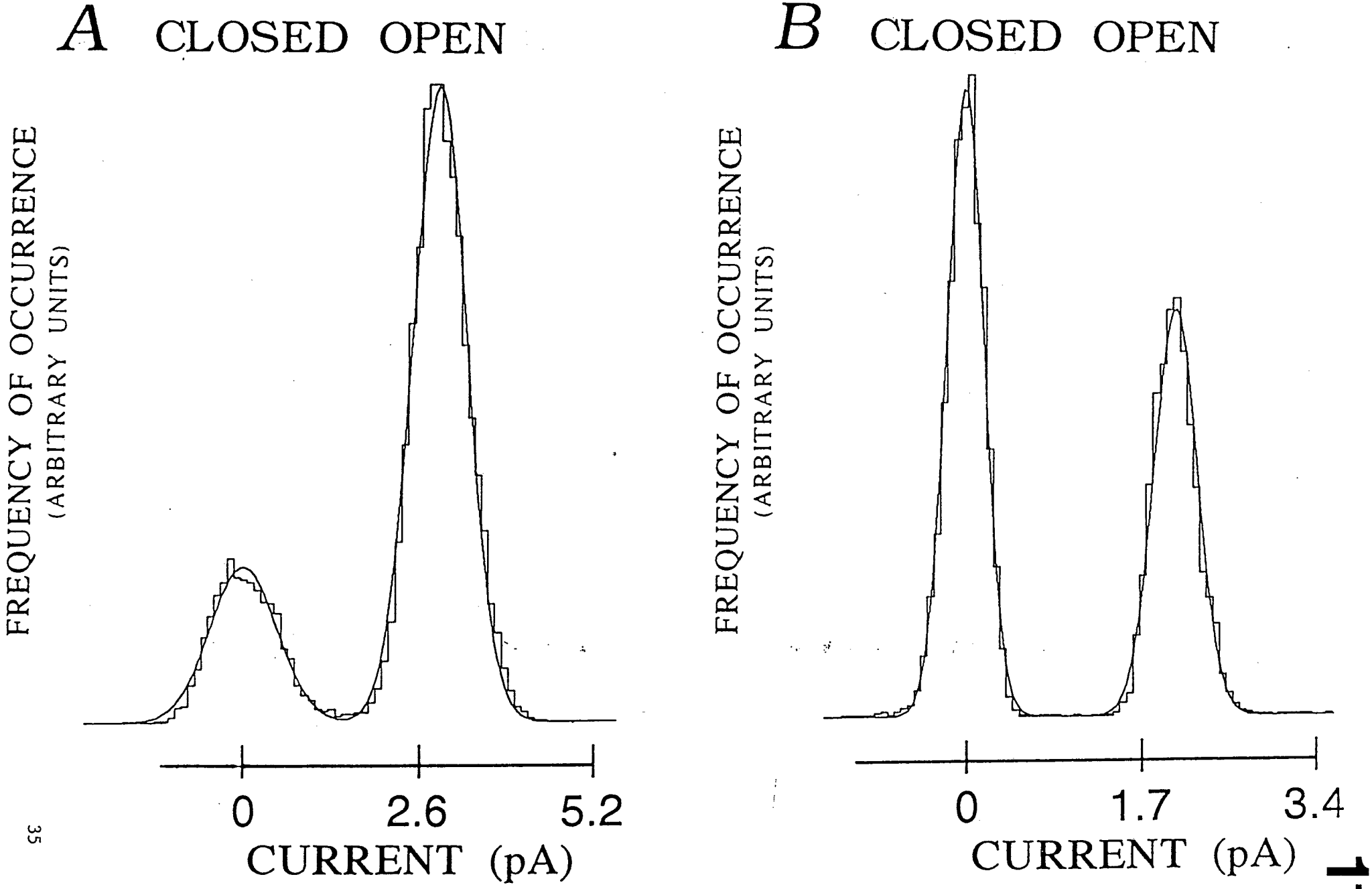
A
CLOSED
OPEN
FREQUENCY OF OCCURRENCE
(ARBITRARY UNITS)
0
2.6
5.2
CURRENT (pA)
B
CLOSED
OPEN
FREQUENCY OF OCCURRENCE
(ARBITRARY UNITS)
0
1.7
3.4
CURRENT (pA)

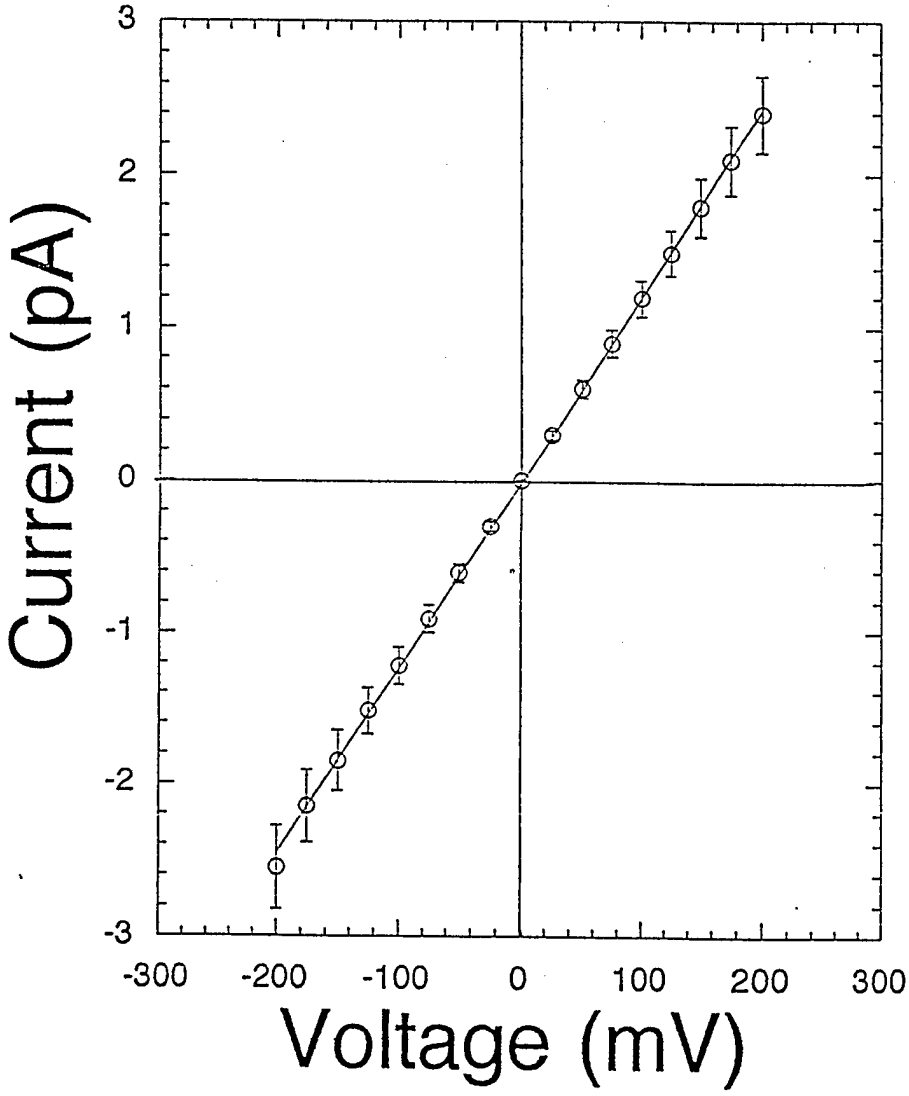
Current (pA)
3
2
1
0
-1
-2
-3
-300
-200
-100
0
100
200
300
Voltage (mV)

PUBLICATIONS THAT HAVE RESULTED FROM THIS FUNDING

Schinder, A. and M. Montal.
Two distinct modalities of NMDA–receptor inactivation induced by calcium influx in rat hippocampal pyramidal neurons.
FEBS Lett. 332:44-48. (1993).

Sun, W., A.V. Ferrer-Montiel and M. Montal.
Primary structure and functional expression of the AMPA/Kainate receptor subunit 2 from human brain.
NeuroReport 5:441-444. (1994).

Montal, M., (Editor).
Reconstitution of membrane transport proteins.
Methods: A Companion to Methods in Enzymology 6:1-2. (1994).

Ferrier-Montiel, A.V. and M. Montal.
Structure–function relations in ligand–gated ion channels: Reconstitution in lipid bilayers and heterologous expression in *Xenopus* oocytes.
Methods: A Companion to Methods in Enzymology 6:60-69. (1994).

Sun, W., A.V. Ferrier-Montiel and M. Montal.
Molecular design of the phencyclidine binding site on glutamate receptors of human brain.
Soc. Neurosci. Abstr. Vol. 20, Part 1, p. 235.(1994).

Montal, M.
Design of molecular function: Channels of Communication.
Annu. Rev. Biophys. Biomol. Struct. 24:31-57. (1995).

Ferrer-Montiel, A.V., C.D. Patten, W. Sun, J. Schiffer, R. Planells-Cases and M. Montal.
The M2 transmembrane segment as a molecular determinant of the ion permeation properties in the superfamily of ligand-gated ion channels.
Biochem. Soc. Trans. 22:S382. (1994).

Schinder, A.F., E. Olson, N.C. Spitzer and M. Montal.
The role of mitochondria in glutamate-induced neurotoxicity.
Biophys. J. 68:A384. (1995).

Oblatt-Montal, M., M. Yamazaki, R. Nelson and M. Montal.
Formation of ion channels in lipid bilayers by a peptide with the predicted transmembrane sequence of botulinum neurotoxin A.
Protein Sci. 4:1490-1497. (1995).

Ferrer-Montiel, A.V., W. Sun and M. Montal.
Molecular design of the N-methyl-D-aspartate receptor binding site for phencyclidine and dizolcipine.
Proc. Natl. Acad. Sci. USA 92:8021-8025. (1995).

Planells-Cases, R., A.V. Ferrer-Montiel, C.D. Patten and M. Montal.
Mutation of conserved negatively-charged residues on the S2 and S3 transmembrane segments of a mammalian K^+ channel selectively modulates channel gating.
Proc. Natl. Acad. Sci. USA 92:9422-9426. (1995).

Montal, M.
Molecular mimicry in channel protein structure.
Curr. Opin. Struct. Biol. 5:501-506. (1995).

Gutierrez, L.M., J.M. Canaves, A.V. Ferrer-Montiel, J.A. Reig, M. Montal and S. Viniegra.
A peptide that mimics the carboxy terminal domain of SNAP-25 blocks calcium-dependent exocytosis in chromaffin cells.
FEBS Lett. 372:39-43. (1995).

Ferrer-Montiel, A.V.F. and M. Montal.
Are ionotropic glutamate receptors pentameric assemblies?
Soc. Neurosci. Abstr. 21, Part 3p. 1991. (1995).

Schubert, U., A.V. Ferrer-Montiel, M. Montal and K. Strebel.
The two biological activities of the human immunodeficiency virus type-1 Vpu protein involve two separable structural domains.
J. Virol.70:809-819 (1996).

Ferrer-Montiel, A.V. and M. Montal.
Pentameric subunit stoichiometry of a neuronal glutamate receptor.
Proc. Natl. Acad. Sci. USA, 93:2741-2744 (1996).

Ferrer-Montiel, A.V.F., W. Sun and M. Montal.
A single tryptophan on M2 of glutamate receptor channels confers high permeability to divalent cations.
Biophys. J. 71: 749-758 (1996).

Ferrer-Montiel, A.V.F., J.M. Canaves, B.R. DasGupta, M.C. Wilson and M. Montal.
Tyrosine phosphorylation modulates the activity of clostridial neurotoxins.
J. Biol. Chem. 271:18322-18325 (1996).

Ferrer-Montiel, A.V.F., M. Oblatt-Montal, J. Canaves, L.M. Gutierrez, R. Nelson, M. Yamazaki and M. Montal.
Botulinum neurotoxins: Design of peptide inhibitors of neurosecretion and identification of the ion channel-forming module.
Bioscience Review (1996) (in press)

Apland, J.P., M.G. Filbert, M. Adler, A.V. Ferrer-Montiel and M. Montal.
Blockade of Ach release at a synapse in *Aplysia* by a peptide that mimics the carboxy-terminal domain of SNAP-25.
Bioscience Review (1996) (in press)

Apland, J.P., M. Adler, A.V. Ferrer-Montiel, M. Montal, and M.G. Filbert.
Blockade of Ach release at a synapse in *Aplysia* by a peptide that mimics the carboxy-terminal domain of SNAP-25.
Soc. Neurosci. Abstr. 22, Part 1p. 783. (1996).

Montal, M.
Protein folds in channel structure.
Curr. Opin. Struct. Biol. 6:499-510 (1996)

Schubert, U., A.V.F. Ferrer-Montiel, M. Oblatt-Montal, P. Henklein, K. Strebel and M. Montal.
Identification of an ion channel activity of the Vpu transmembrane domain and its involvement in the regulation of virus release from HIV-1-infected cells.
FEBS Lett. 398:12-18 (1996)

Schinder, A., E. Olson, N.C. Spitzer and M. Montal.
Mitochondrial dysfunction is a primary event in glutamate neurotoxicity.
J. Neurosci. 16:6125-6133 (1996)

Gutierrez, L.M., S. Viniegra, J. Rueda, A.V. Ferrer-Montiel, J.M. Canaves and M. Montal.
A peptide that mimics the C-terminal sequence of SNAP-25 inhibits secretory vesicle docking in chromaffin cells.
J. Biol. Chem. 272:2634-2639 (1997)

PERSONNEL RECEIVING PAY FROM THE NEGOTIATED EFFORT

Mauricio Montal	Professor of Biology, Principal Investigator
Antonio Ferrer-Montiel	Assistant Project Scientist
Myrta Oblatt-Montal	Staff Research Associate
Rosa Planells-Cases	Graduate Student
Alejandro Schinder	Graduate Student
Craig D. Patten	Graduate Student
Jaime Merino	Postgraduate Research Biologist
Anh Tonnu	Laboratory Assistant
Carrie Smith	Laboratory Assistant
Arlene Kelly	Laboratory Assistant
Sarah Tung	Laboratory Assistant
Zachary Wilkinson	Laboratory Assistant
Timothy Shum	Laboratory Assistant
Pei Cheng	Laboratory Assistant